Electronic Supplementary Material (ESI) for Green Chemistry.

SUPPORTING INFORMATION

Visible-Light-Induced Aerobic Oxidation of Alcohols to Aldehydes/Ketones via Solvated Dispersion Intermediates

Wenlong Lei, Runze Liu, Rengui Li, Yan Liu, Can Li *

Contents

General experimental details

Commercially available reagents were used without further purification. Analytical grade solvents and commercially available reagents were used to conduct the reactions. 40 wt% hydrogen bromide aqueous solution (HBr); 37 wt.% hydrochloric acid aqueous solution (HCl), 57 wt.% hydriodic acid aqueous solution (HI); 40 wt.% sulfuric acid aqueous solution (H_2SO_4). Unless otherwise stated, all reactions were set up in a clear quartz vessel and were stirred with a Teflon-coated magnetic stir bar. Reactions were conducted with visible light irradiation ≥ 420 nm (300W Microsolar 300 series xenon light source as light source). Gas chromatograph (GC) measurements were carried out in an Agilent 7890 GC with a flame ionization detector was used to quantify the products, equipping with a HP-5 column (30 m^3 x 0.320 mm^3 x 0.25 mm). GC-MS analysis (Agilent 7890 GC, interfaced with 5975C MS, USA). The thin layer chromatography (TLC) analyses were performed using silica gel glass plates, and the products were obtained by column chromatography on silica gel (200-300 mesh) or aluminum oxide neutral (200-300 mesh). NMR spectra were recorded on Bruker AM-400 MHz or AM-700 MHz spectrometer for proton and carbon magnetic resonance spectra (^{1}H NMR and ^{13}C NMR) in the solvent of deuterated chloroform ($CDCl_3$). $CDCl_3$: ^{1}H NMR: δ 7.26 ppm, singlet peak; ^{13}C NMR: δ 77.16 ppm, triplet peak. In reporting spectral data the format (δ) chemical shift (multiplicity, J values in Hz, integration) was used with the following abbreviations: s = singlet, d = doublet, t = triplet, q = quartet, quint = quintuplet, m = multiplet. UV-visible data were recorded over the spectral range of 200-700 nm on a UV-vis spectrophotometer (JASCO V-650) equipped with an integrating sphere. MS data was obtained with Agilent 6540 Accurate-MS spectrometer (Q-TOF). Electron paramagnetic resonance (EPR) spectra were collected on a Bruker EPR A200 spectrometer under ambient conditions. The possible metal residues in the reaction systems are detected by Inductively Coupled Plasma Optical Emission Spectroscopy (ICP-OES), includes all reagents, substrates, glass-wares, and even stir-bars. ICP-OES analysis was performed with Thermo ICP-OES 7300DV (PerkinElmer).

Conditions optimization.

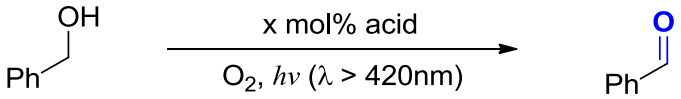

Visible light-induced benzyl alcohol conversion: We commenced the photo-induced aerobic alcohol oxidation using benzyl alcohol (BnOH) and O_2 as oxidant with different acids and solvents at ambient temperature under visible light irradiation ($\lambda \geq 420$ nm). The cylinder reactor is about 80 mm high and 50 mm diameter. The reaction is carry out under O_2 with sealed reactor. The distance of the light source is about 30 cm.

In a clear quartz bottle with a rubber septum and magnetic stirring bar, BnOH (0.1 mmol) and x mol% different acids were added into the 6.0 mL reaction solvent under visible-light irradiation $\lambda \geq 420$ nm, the reaction mixture was stirred under ambient conditions. In the reaction progress was monitored via GC thin layer chromatography or (TLC). The product was determined and analyzed by a gas chromatograph (GC, 7890, Agilent) with a thermal conductivity detector (TCD) and a flame ionization detector (FID), or nuclear magnetic resonance (NMR) spectroscopy.

General procedure for the photocatalytic aerobic oxidation alcohol

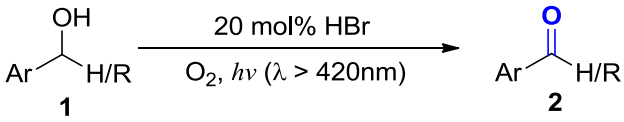

The experimental procedure: In a clear quartz bottle with a rubber septum and magnetic stirring bar, substrate (0.2 mmol), 20 mol% HBr were added into the 12.0 mL EtOAc as solvent under visible-light irradiation ≥ 420 nm, the reaction mixture was stirred under ambient conditions. In the reaction progress can be monitored via GC or TLC. After completion of the reaction, the solvent was removed in vacuo or extraction and the residue was purified by chromatography column on silica gel by petroleum ether/EtOAc to

give the desired product. The some sample was determined and analyzed by GC-FID, using chlorobenzene as internal standard. The PhCHO selectivity refers to overoxidation to benzoic acid.

We commenced the photo-induced aerobic alcohol oxidation using benzyl alcohol (BnOH) and O_2 as oxidant with different acids and solvents at ambient temperature under visible light irradiation ($\lambda \geq 420$ nm). The cylinder reactor is about 80 mm high and 50 mm diameter. The reaction is carry out under O_2 with sealed reactor.The distance of the light source is about 30 cm.

UV/Vis absorption spectra

UV/vis absorption spectra between benzyl alcohol and HBr in EtOAc were recorded in path quartz cuvettes using UV-vis spectrophotometer (JASCO V-650).

As shown in Figure 2a, experimental procedure:

Br_2: 0.02 mmol Bromine in 3.0 mL EtOAc

HBr(dark): 0.02 mmol HBr in 3.0 mL EtOAc

HBr(Vis): 0.02 mmol HBr in 3.0 mL EtOAc at 10 minutes under visible-light irradiation≥ 420 nm

HBr(UV): 0.02 mmol HBr in 3.0 mL EtOAc at 10 minutes under visible-light irradiation≥ 320 nm

As shown in Figure 2b, experimental procedure:

BnOH(dark): 0.1 mmol benzyl alcohol in 6.0 mL EtOAc

BnOH+HBr (dark): 0.1 mmol benzyl alcohol and 20 mol% HBr in 6.0 mL EtOAc

BnOH+HBr (Vis): 0.1 mmol benzyl alcohol and 20 mol% HBr in 6.0 mL EtOAc at 3 minutes under visible-light irradiation $\lambda \geq 420$ nm

The Tyndall effect.

Using EtOAc solvent observed the Tyndall effect

1-Pyrenemethanol (0.1 mmol) and 20 mol% HBr were adding in 3.0 mL EtOAc, we did not observe the Tyndall effect. Introducing 3.0 mL ETOAC into the solution, the Tyndall effect was observed.

Using CH_2Cl_2 solvent observed the Tyndall effect

In order to compare the influence of different solvents on the Tyndall effect, CH_2Cl_2 was used as the reaction solvent. 1-Pyrenemethanol (0.1mmol) and 20 mol% HBr were adding in 3.0 mL CH_2Cl_2, we did not observe the Tyndall effect. Introducing 1.0 mL EtOAc into the solution, the Tyndall effect was observed.

Selectivity and conversion of benzyl alcohol oxidation in EtOAc/CH_2Cl_2 ratios

Experimental procedure: In a clear quartz bottle with a rubber septum and magnetic stirring bar, benzyl alcohol (0.2 mmol), 20 mol% HBr, were added into the 12 mL the mixing solvent EtOAc/CH_2Cl_2 under visible-light irradiation≥ 420 nm. The constant total volume stoichiometry is 12.0 mL. The different volume ratios of EtOAc/CH_2Cl_2 were 10:0, 9:1, 8:2, 6:4, 5:5, 0:10 respectively. The product yield was determined by GC.

EPR study

EPR spectrum was measured on a Bruker ER200DSRC10/12 EPR spectrometer by using DMPO (5,5-dimethyl-1-pyrroline-1-oxide) as a standard.

Experimental procedure: In a clear flame-dried quartz bottle with a rubber septum and magnetic stirring bar, benzyl alcohol (0.2 mmol), 20 mol% HBr were added into the 12.0 mL EtOAc as solvent. The reaction mixture was stirred under ambient conditions under

visible-light irradiation ≥ 420 nm. After 5 min, DMPO (0.3 mmol) and K_2CO_3 (0.2 mmol) were added. The sample was detected via EPR.

Quenching Experiments for the Photo-oxidation of Benzyl Alcohol.

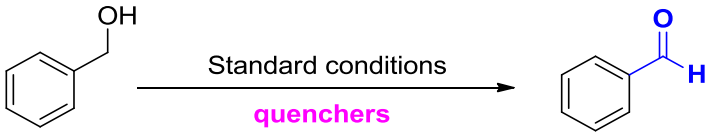

In a clear quartz bottle with a rubber septum and magnetic stirring bar, substrate (0.1 mmol), 20 mol% HBr, quenchers (0.15 mmol) were added into the 6.0 mL EtOAc as solvent under visible-light irradiation≥ 420 nm. The presence of different scavengers: No scavenger (Blank), TEMPO, BHT, BQ, $CuCl_2$. The reaction mixture was stirred under ambient conditions. After 15 min, the reaction mixture sample was determined and analyzed by GC-FID.

DFT calculation

Computational methods

In the present work, all electronic structure calculations were performed using the Gaussian 16 program suite.[1] Geometry optimizations were carried out based on DFT description for the ground state and TD-DFT descriptions for the excited states. Solvent effects of EtOAc were implicitly taken into account by employing the solvation model based on density (SMD).[2] The (U)CAM-B3LYP[3] functional with TZVP[4] basis set and Grimme's D3[5] dispersion correction (Becke-Johnson damping) was employed in both the DFT and TD-DFT calculations to properly consider dispersion interactions[6] as well as excited states with charge transfer characters.[7] The nature of the optimized stationary points was characterized by the frequency calculations. The wavefunctions for all calculations have been optimized to stabilization for a rational description of open-shell electronic structures. Electrostatic potential (ESP) analysis and charge transfer for excited

state transition was computed with the Multiwfn package.[8] Conical section optimization of the ground and first excited state was performed using TD-DFT method at the same level of theory implemented by ORCA 5.0 package suite.[9]

Supplementary Figures and Tables

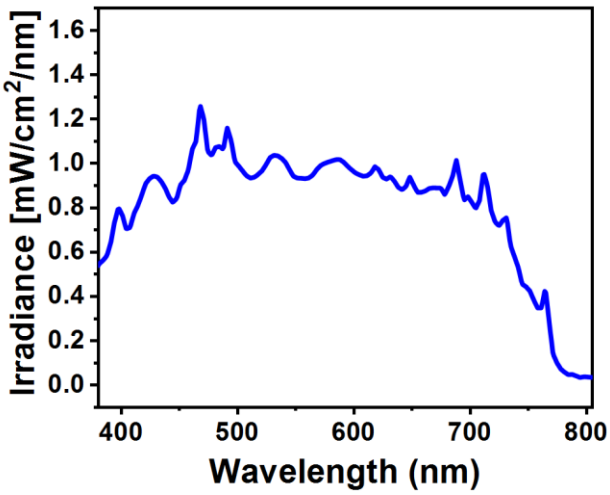

Figure S1 The irradiation output spectrum of light setup in the reaction.

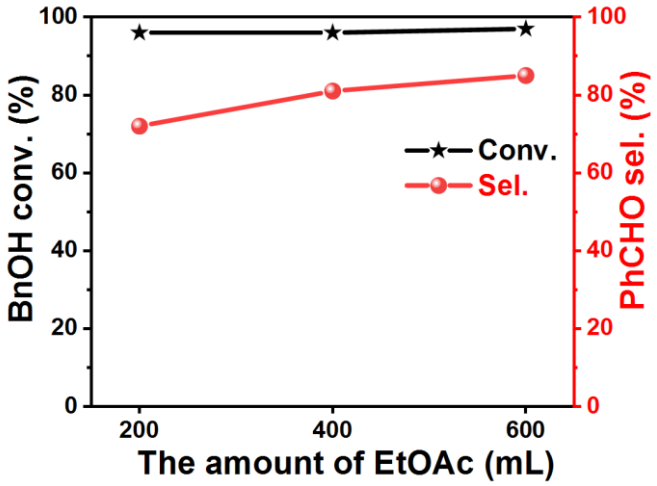

Figure S2. Performance of the reaction with the solvent dosage of EtOAc.

The experimental procedure: In a clear pyrex glass beaker with a rubber septum and magnetic stirring bar, benzyl alcohol (10 mmol, 1.08 g), 20 mol% HBr were added into 200, 400 or 600 mL EtOAc as solvent under visible-light irradiation ≥ 420 nm, the reaction mixture was stirred at ambient conditions. The reaction was monitored by TLC or GC.

(a) Mean Data: 1608 leiwenlong 2#

Analyte	Mean Corrected Intensity	Calib. Conc.	Units	Std. Dev.	Sample Conc.	Units	Std. Dev.	RSD
As 228.812	61.0	0.003	mg/L	0.0002	0.003	mg/L	0.0002	6.57%
Be 313.107	-162.2	-0.001	mg/L	0.0001	-0.001	mg/L	0.0001	9.47%
Cd 228.802	61.9	0.003	mg/L	0.0002	0.003	mg/L	0.0002	5.64%
Cr 267.716	15.1	0.001	mg/L	0.0006	0.001	mg/L	0.0006	43.45%
Co 228.616	1.2	0.001	mg/L	0.0006	0.001	mg/L	0.0006	66.61%
Cu 327.393	52.8	0.001	mg/L	0.0004	0.001	mg/L	0.0004	23.89%
Fe 238.204	-202.7	-0.003	mg/L	0.0002	-0.003	mg/L	0.0002	6.34%
Pb 220.353	54.0	0.009	mg/L	0.0071	0.009	mg/L	0.0071	78.00%
Mn 257.610	-51.8	-0.008	mg/L	0.0001	-0.008	mg/L	0.0001	1.28%
Mo 202.031	-47.3	-0.001	mg/L	0.0020	-0.001	mg/L	0.0020	149.85%
Ni 231.604	94.6	0.003	mg/L	0.0005	0.003	mg/L	0.0005	15.64%
Sb 206.836	8.9	0.007	mg/L	0.0048	0.007	mg/L	0.0048	66.89%
Se 196.026	400.7	0.296	mg/L	0.0188	0.296	mg/L	0.0188	6.35%
Sr 407.771	23.6	0.002	mg/L	0.0005	0.002	mg/L	0.0005	21.97%
Ti 334.940	-157.6	-0.001	mg/L	0.0000	-0.001	mg/L	0.0000	2.81%
V 290.880	-71.8	0.004	mg/L	0.0013	0.004	mg/L	0.0013	34.33%
Zn 206.200	-0.8	-0.001	mg/L	0.0010	-0.001	mg/L	0.0010	125.49%
Ba 233.527	38.5	-0.008	mg/L	0.0002	-0.008	mg/L	0.0002	2.08%
Ag 328.068	-17.8	-0.005	mg/L	0.0002	-0.005	mg/L	0.0002	4.48%
Ce 413.764	-2663.9	-0.004	mg/L	0.0002	-0.004	mg/L	0.0002	5.83%
Sm 359.260	-491.3	-0.003	mg/L	0.0001	-0.003	mg/L	0.0001	3.33%
Ru 240.272	-32.7	-0.000	mg/L	0.0002	-0.000	mg/L	0.0002	111.40%
Au 267.595	38.4	0.000	mg/L	0.0011	0.000	mg/L	0.0011	502.21%
Pd 340.458	13.0	0.000	mg/L	0.0002	0.000	mg/L	0.0002	450.97%
Pt 265.945	-93.8	-0.001	mg/L	0.0014	-0.001	mg/L	0.0014	102.91%
Rh 343.489	328.6	0.001	mg/L	0.0007	0.001	mg/L	0.0007	64.16%
In 325.609	56.8	0.002	mg/L	0.0007	0.002	mg/L	0.0007	29.30%
U 385.958	-2296.4	-0.024	mg/L	0.0018	-0.024	mg/L	0.0018	7.51%
Re 227.525	-248.6	-0.002	mg/L	0.0001	-0.002	mg/L	0.0001	6.56%

(b) Mean Data: 1608 leiwenlong 3#

Analyte	Mean Corrected Intensity	Calib. Conc.	Units	Std. Dev.	Sample Conc.	Units	Std. Dev.	RSD
As 228.812	34.2	0.002	mg/L	0.0007	0.002	mg/L	0.0007	31.94%
Be 313.107	-495.6	-0.001	mg/L	0.0001	-0.001	mg/L	0.0001	9.64%
Cd 228.802	33.6	0.002	mg/L	0.0007	0.002	mg/L	0.0007	32.43%
Cr 267.716	47.1	0.002	mg/L	0.0005	0.002	mg/L	0.0005	31.08%
Co 228.616	30.7	0.002	mg/L	0.0011	0.002	mg/L	0.0011	68.91%
Cu 327.393	6.2	0.001	mg/L	0.0007	0.001	mg/L	0.0007	59.95%
Fe 238.204	-179.9	-0.003	mg/L	0.0001	-0.003	mg/L	0.0001	4.98%
Pb 220.353	10.9	0.002	mg/L	0.0110	0.002	mg/L	0.0110	666.38%
Mn 257.610	-115.9	-0.008	mg/L	0.0000	-0.008	mg/L	0.0000	0.17%
Mo 202.031	39.5	0.004	mg/L	0.0020	0.004	mg/L	0.0020	45.65%
Ni 231.604	42.1	0.002	mg/L	0.0009	0.002	mg/L	0.0009	55.80%
Sb 206.836	-0.6	0.005	mg/L	0.0071	0.005	mg/L	0.0071	153.41%
Se 196.026	58.6	0.049	mg/L	0.0228	0.049	mg/L	0.0228	46.30%
Sr 407.771	-40.2	0.002	mg/L	0.0001	0.002	mg/L	0.0001	5.70%
Ti 334.940	-273.1	-0.002	mg/L	0.0000	-0.002	mg/L	0.0000	1.28%
V 290.880	222.3	0.006	mg/L	0.0008	0.006	mg/L	0.0008	14.22%
Zn 206.200	-33.6	-0.002	mg/L	0.0007	-0.002	mg/L	0.0007	36.51%
Ba 233.527	11.8	-0.008	mg/L	0.0002	-0.008	mg/L	0.0002	3.07%
Ag 328.068	31.4	-0.005	mg/L	0.0005	-0.005	mg/L	0.0005	10.09%
Ce 413.764	-1534.6	-0.002	mg/L	0.0004	-0.002	mg/L	0.0004	20.32%
Sm 359.260	-132.2	-0.003	mg/L	0.0003	-0.003	mg/L	0.0003	10.30%
Ru 240.272	-108.9	-0.001	mg/L	0.0001	-0.001	mg/L	0.0001	11.03%
Au 267.595	-14.5	-0.000	mg/L	0.0002	-0.000	mg/L	0.0002	262.41%
Pd 340.458	28.4	0.000	mg/L	0.0003	0.000	mg/L	0.0003	230.66%
Pt 265.945	-118.9	-0.002	mg/L	0.0004	-0.002	mg/L	0.0004	26.02%
Rh 343.489	559.5	0.002	mg/L	0.0006	0.002	mg/L	0.0006	29.97%
In 325.609	18.9	0.002	mg/L	0.0018	0.002	mg/L	0.0018	107.00%
U 385.958	-138.4	-0.001	mg/L	0.0006	-0.001	mg/L	0.0006	45.74%
Re 227.525	-24.3	-0.000	mg/L	0.0001	-0.000	mg/L	0.0001	86.88%

(c) Mean Data: 1608 leiwenlong 4#

Analyte	Mean Corrected Intensity	Calib. Conc.	Units	Std. Dev.	Sample Conc.	Units	Std. Dev.	RSD
As 228.812	3.8	0.002	mg/L	0.0009	0.002	mg/L	0.0009	49.29%
Be 313.107	-311.7	-0.001	mg/L	0.0001	-0.001	mg/L	0.0001	9.71%
Cd 228.802	6.7	0.002	mg/L	0.0009	0.002	mg/L	0.0009	48.81%
Cr 267.716	-10.4	0.001	mg/L	0.0006	0.001	mg/L	0.0006	63.28%
Co 228.616	41.2	0.002	mg/L	0.0008	0.002	mg/L	0.0008	44.77%
Cu 327.393	118.2	0.002	mg/L	0.0002	0.002	mg/L	0.0002	7.97%
Fe 238.204	-119.1	-0.002	mg/L	0.0005	-0.002	mg/L	0.0005	22.44%
Pb 220.353	8.3	0.001	mg/L	0.0021	0.001	mg/L	0.0021	171.74%
Mn 257.610	-86.2	-0.008	mg/L	0.0000	-0.008	mg/L	0.0000	0.57%
Mo 202.031	-26.6	0.000	mg/L	0.0009	0.000	mg/L	0.0009	>999.9%
Ni 231.604	98.4	0.003	mg/L	0.0006	0.003	mg/L	0.0006	17.29%
Sb 206.836	-26.0	-0.002	mg/L	0.0057	-0.002	mg/L	0.0057	236.76%
Se 196.026	23.7	0.024	mg/L	0.0098	0.024	mg/L	0.0098	41.00%
Sr 407.771	-51.8	0.002	mg/L	0.0001	0.002	mg/L	0.0001	6.97%
Ti 334.940	-229.2	-0.002	mg/L	0.0001	-0.002	mg/L	0.0001	7.05%
V 290.880	-245.1	0.003	mg/L	0.0007	0.003	mg/L	0.0007	27.76%
Zn 206.200	2.9	-0.001	mg/L	0.0010	-0.001	mg/L	0.0010	148.03%
Ba 233.527	45.8	-0.007	mg/L	0.0000	-0.007	mg/L	0.0000	0.46%
Ag 328.068	58.5	-0.005	mg/L	0.0001	-0.005	mg/L	0.0001	2.78%
Ce 413.764	-942.9	-0.001	mg/L	0.0014	-0.001	mg/L	0.0014	125.05%
Sm 359.260	-113.7	-0.003	mg/L	0.0002	-0.003	mg/L	0.0002	6.43%
Ru 240.272	-82.2	-0.001	mg/L	0.0007	-0.001	mg/L	0.0007	134.01%
Au 267.595	-89.4	-0.001	mg/L	0.0002	-0.001	mg/L	0.0002	36.01%
Pd 340.458	46.9	0.000	mg/L	0.0002	0.000	mg/L	0.0002	108.38%
Pt 265.945	-137.8	-0.002	mg/L	0.0006	-0.002	mg/L	0.0006	28.85%
Rh 343.489	518.4	0.002	mg/L	0.0003	0.002	mg/L	0.0003	14.61%
In 325.609	110.6	0.003	mg/L	0.0008	0.003	mg/L	0.0008	28.43%
U 385.958	-2883.9	-0.030	mg/L	0.0014	-0.030	mg/L	0.0014	4.66%
Re 227.525	-54.8	-0.000	mg/L	0.0002	-0.000	mg/L	0.0002	54.38%

(d) Mean Data: 1608 leiwenlong 5#

Analyte	Mean Corrected Intensity	Calib. Conc.	Units	Std. Dev.	Sample Conc.	Units	Std. Dev.	RSD
As 228.812	8.0	0.002	mg/L	0.0002	0.002	mg/L	0.0002	8.96%
Be 313.107	-254.3	-0.001	mg/L	0.0001	-0.001	mg/L	0.0001	6.86%
Cd 228.802	9.5	0.002	mg/L	0.0001	0.002	mg/L	0.0001	7.18%
Cr 267.716	-2.3	0.001	mg/L	0.0007	0.001	mg/L	0.0007	71.92%
Co 228.616	65.3	0.002	mg/L	0.0006	0.002	mg/L	0.0006	24.09%
Cu 327.393	158.3	0.002	mg/L	0.0004	0.002	mg/L	0.0004	18.20%
Fe 238.204	-149.3	-0.003	mg/L	0.0005	-0.003	mg/L	0.0005	20.56%
Pb 220.353	7.8	0.001	mg/L	0.0056	0.001	mg/L	0.0056	500.11%
Mn 257.610	-131.6	-0.008	mg/L	0.0001	-0.008	mg/L	0.0001	1.11%
Mo 202.031	-24.3	0.000	mg/L	0.0003	0.000	mg/L	0.0003	119.51%
Ni 231.604	8.1	0.001	mg/L	0.0010	0.001	mg/L	0.0010	159.77%
Sb 206.836	4.2	0.006	mg/L	0.0033	0.006	mg/L	0.0033	56.58%
Se 196.026	2.3	0.009	mg/L	0.0177	0.009	mg/L	0.0177	206.66%
Sr 407.771	-30.7	0.002	mg/L	0.0001	0.002	mg/L	0.0001	3.58%
Ti 334.940	-248.9	-0.002	mg/L	0.0001	-0.002	mg/L	0.0001	5.58%
V 290.880	-310.3	0.002	mg/L	0.0013	0.002	mg/L	0.0013	58.43%
Zn 206.200	7.8	-0.000	mg/L	0.0009	-0.000	mg/L	0.0009	179.04%
Ba 233.527	39.6	-0.008	mg/L	0.0002	-0.008	mg/L	0.0002	2.25%
Ag 328.068	88.7	-0.005	mg/L	0.0003	-0.005	mg/L	0.0003	5.66%
Ce 413.764	-3196.4	-0.005	mg/L	0.0002	-0.005	mg/L	0.0002	3.20%
Sm 359.260	-330.5	-0.003	mg/L	0.0004	-0.003	mg/L	0.0004	12.87%
Ru 240.272	-127.6	-0.001	mg/L	0.0005	-0.001	mg/L	0.0005	60.18%
Au 267.595	-60.2	-0.000	mg/L	0.0002	-0.000	mg/L	0.0002	51.72%
Pd 340.458	36.1	0.000	mg/L	0.0004	0.000	mg/L	0.0004	233.41%
Pt 265.945	-98.0	-0.001	mg/L	0.0005	-0.001	mg/L	0.0005	32.05%
Rh 343.489	220.2	0.001	mg/L	0.0009	0.001	mg/L	0.0009	126.70%
Re 227.525	-241.4	-0.002	mg/L	0.0003	-0.002	mg/L	0.0003	17.37%

(e) Mean Data: 1608 leiwenlong 6#

Analyte	Mean Corrected Intensity	Calib. Conc.	Units	Std. Dev.	Sample Conc.	Units	Std. Dev.	RSD
As 228.812	-22.6	0.001	mg/L	0.0001	0.001	mg/L	0.0001	6.62%
Be 313.107	-394.5	-0.001	mg/L	0.0000	-0.001	mg/L	0.0000	2.84%
Cd 228.802	-25.0	0.001	mg/L	0.0000	0.001	mg/L	0.0000	3.36%
Cr 267.716	-25.2	0.001	mg/L	0.0009	0.001	mg/L	0.0009	126.11%
Co 228.616	87.8	0.003	mg/L	0.0007	0.003	mg/L	0.0007	24.66%
Cu 327.393	108.8	0.002	mg/L	0.0008	0.002	mg/L	0.0008	43.96%
Fe 238.204	-201.0	-0.003	mg/L	0.0003	-0.003	mg/L	0.0003	10.52%
Pb 220.353	-30.5	-0.005	mg/L	0.0040	-0.005	mg/L	0.0040	73.43%
Mn 257.610	-104.9	-0.008	mg/L	0.0000	-0.008	mg/L	0.0000	0.54%
Mo 202.031	-10.2	0.001	mg/L	0.0011	0.001	mg/L	0.0011	92.13%
Ni 231.604	30.7	0.001	mg/L	0.0010	0.001	mg/L	0.0010	76.20%
Sb 206.836	2.7	0.005	mg/L	0.0062	0.005	mg/L	0.0062	112.87%
Se 196.026	23.4	0.024	mg/L	0.0207	0.024	mg/L	0.0207	87.08%
Sr 407.771	23.9	0.002	mg/L	0.0002	0.002	mg/L	0.0002	9.34%
Ti 334.940	-319.8	-0.002	mg/L	0.0001	-0.002	mg/L	0.0001	8.27%
V 290.880	-331.9	0.002	mg/L	0.0012	0.002	mg/L	0.0012	59.50%
Zn 206.200	40.4	0.001	mg/L	0.0004	0.001	mg/L	0.0004	69.59%
Ba 233.527	51.1	-0.007	mg/L	0.0002	-0.007	mg/L	0.0002	3.18%
Ag 328.068	-54.4	-0.006	mg/L	0.0005	-0.006	mg/L	0.0005	9.43%
Ce 413.764	-1533.9	-0.002	mg/L	0.0005	-0.002	mg/L	0.0005	25.27%
Sm 359.260	-119.4	-0.003	mg/L	0.0002	-0.003	mg/L	0.0002	6.27%
Ru 240.272	-30.5	-0.000	mg/L	0.0003	-0.000	mg/L	0.0003	152.54%
Au 267.595	-69.4	-0.000	mg/L	0.0005	-0.000	mg/L	0.0005	118.89%
Pd 340.458	22.2	0.000	mg/L	0.0001	0.000	mg/L	0.0001	159.74%
Pt 265.945	-136.8	-0.002	mg/L	0.0011	-0.002	mg/L	0.0011	53.74%
Rh 343.489	680.0	0.002	mg/L	0.0004	0.002	mg/L	0.0004	17.00%
In 325.609	-55.3	0.001	mg/L	0.0014	0.001	mg/L	0.0014	197.67%
U 385.958	-91.9	-0.001	mg/L	0.0016	-0.001	mg/L	0.0016	206.62%
Re 227.525	-87.2	-0.001	mg/L	0.0002	-0.001	mg/L	0.0002	32.19%

Figure S3 The analysis of residual metal contents by ICP-OES: (a) reaction solution (b) BnOH (c) HBr (d) EtOAc (e) glasswares and stirbars in water solvent.

Table S1. Control experiments.

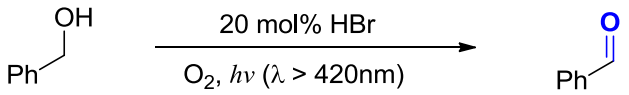

Entry[a]	catalyst	Conversion [%][b]	selectivity[%][b]
1	HBr	93	97
2	No O_2	-	-
3	No *hv*	-	-
4	No Br^- (40 wt% H_2SO_4 instesd of HBr)	-	-
5	No Br^- (HCl instesd of HBr)	-	-
6	No Br^- (HI instesd of HBr)	18	> 90
7	No H^+ (KBr instesd of HBr)	-	-
8	No H^+ (NBu_4Br instesd of HBr)	-	-
9	10 mol% H_2O instesd of HBr	-	-
10	20 mol% H_2O instesd of HBr	-	-
11	40 mol% H_2O instesd of HBr	-	-
12	80 mol% H_2O instesd of HBr	-	-
13	20 mol% HCl and 63 mol% H_2O	-	-
14	20 mol% HI and 27 mol% H_2O	16	98

[a] Reaction conditions: benzyl alcohol (0.1 mmol), 20 mol% HBr or others, 6.0 mL solvent, under ambient conditions, reaction time: 15 min, visible light irradiation ≥ 420 nm. [b] Products were quantified by GC with chlorobenzene as an internal standard.

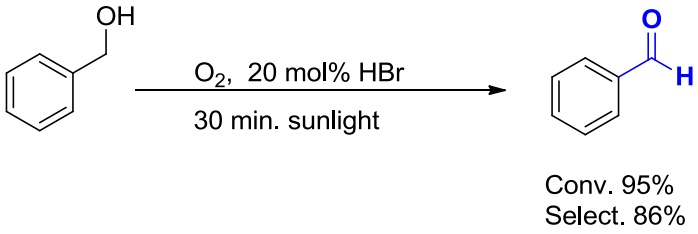

Figure S4: The photoinduced aerobic oxidation of alcohol by sunlight and the reaction setup

The experimental procedure: In a clear quartz bottle with a rubber septum and magnetic stirring bar, benzyl alcohol (0.2 mmol), 20 mol% HBr were added into the 12.0 mL EtOAc as solvent under sunlight, the reaction mixture was stirred under ambient conditions. In the reaction progress was monitored via GC.

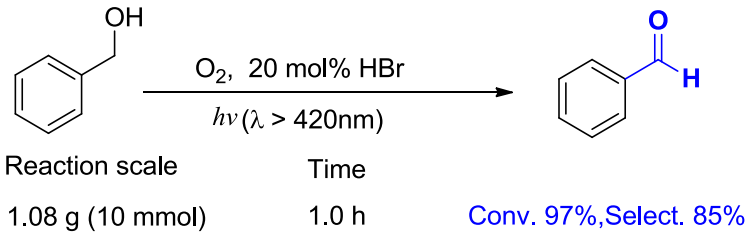

Figure S5: Gram-scale synthesis of benzaldehyde

The experimental procedure: In a clear pyrex glass beaker with a rubber septum and magnetic stirring bar, benzyl alcohol (10 mmol, 1.08 g), 20 mol% HBr were added into 600 mL EtOAc as solvent under visible-light irradiation ≥ 420 nm, the reaction mixture was stirred at ambient conditions. The reaction was monitored by TLC or GC. After completion of the reaction, it was determined using GC.

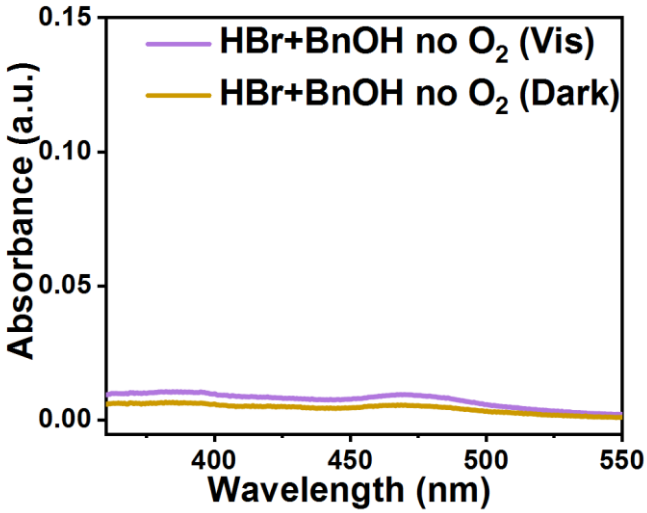

Figure S6 The UV-vis spectra of HBr and BnOH without O_2 under irradiation (visible light) and in dark.

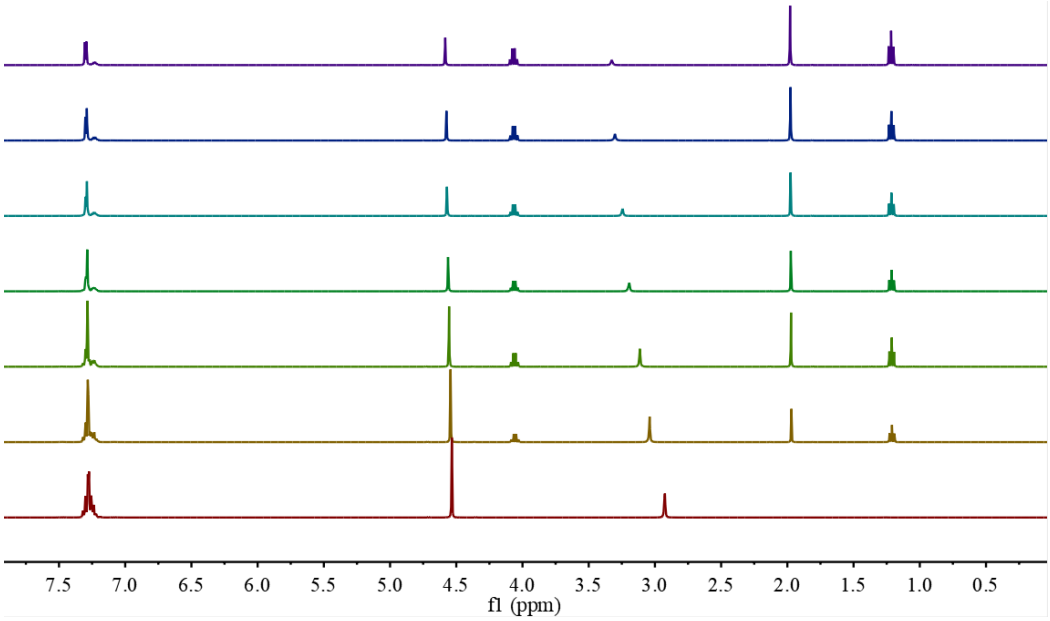

Figure S7: The ^{1}HNMR titration of increasing amounts of EtOAc (bottom to top) into a solution of benzyl alcohol.

^{1}H titrations between benzyl alcohol and EtOAc：The concentration of benzyl alcohol was 1.23 mM in $CDCl_3$ and concentrations of EtOAc were 0 mM, 0.246 mM, 0.615 mM, 0.923 mM, 1.23 mM, 1.54 mM, 1.85 mM.

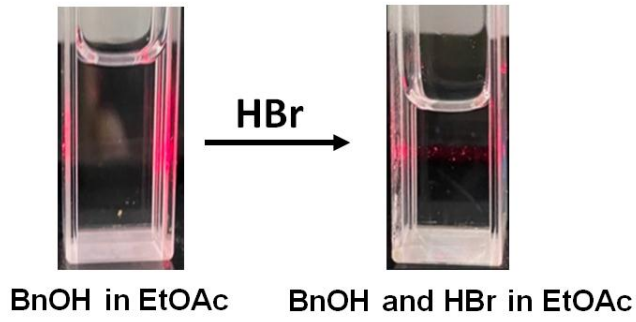

Figure S8 Using benzyl alcohol as reactant to detect Tyndall effect.

In order to detect the Tyndall effect, ethyl acetate (EtOAc) was used as the reaction solvent. Benzyl alcohol (0.1mmol) was adding in 3.0 mL EtOAc, we did not observe the Tyndall effect. Introducing 20 mol% HBr into the solution, the Tyndall effect was observed.

Figure S9. Tests on Tyndall effect: HBr and BnOH in acetone solution

In order to detect the Tyndall effect, acetone was used as the reaction solvent. Benzyl alcohol (0.1mmol) and 20 mol% HBr were adding in acetone solution.

The carbonyl groups of ethyl acetate or acetone solvent both seem to form hydrogen bonds with the substrates of alcohol –OH groups, but the reaction performance and Tyndall effect show different, which may be due to the differences in hydrophilicity, polarity and solvent effects of the two solvents.[10, 11]

Figure S10. Tests on Tyndall effect: H_2O and BnOH in EtOAc solution

In order to detect the Tyndall effect, EtOAc was used as the reaction solvent. Benzyl alcohol (0.1mmol) and 20 mol% H_2O were adding in EtOAc solution.

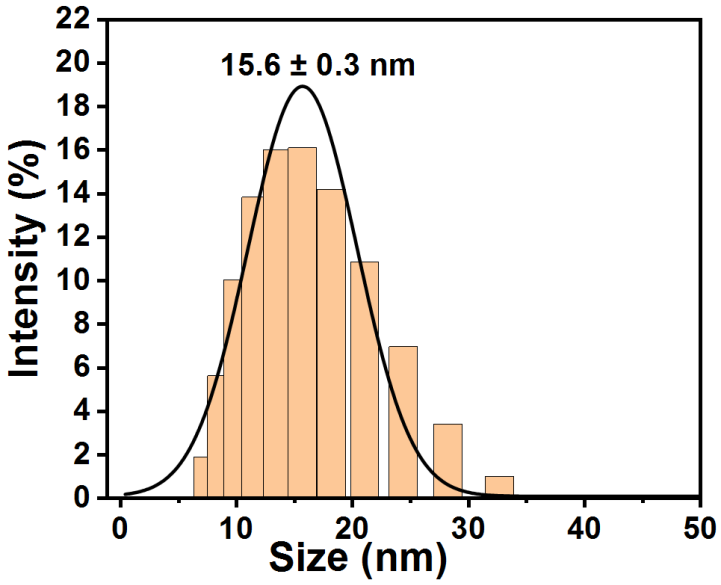

Figure S11 The size distribution

Experimental procedure: 1-Pyrenemethanol and 20 mol% HBr based on 1-Pyrenemethanol were adding in 6.0 mL EtOAc.

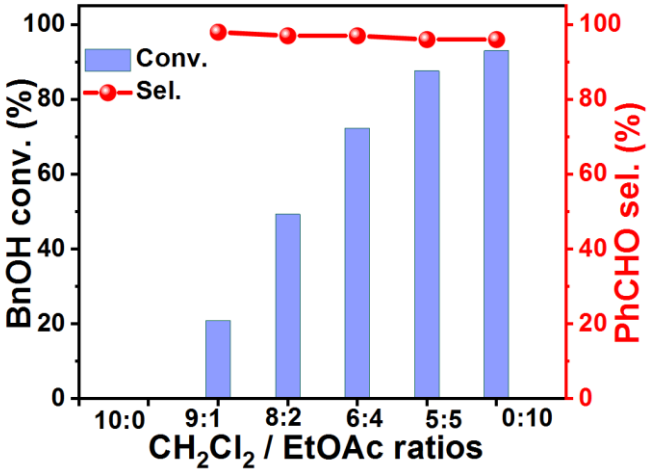

Figure 12 Selectivity and conversion of BnOH in the mixed solvent of EtOAc and CH_2Cl_2 in different proportions.

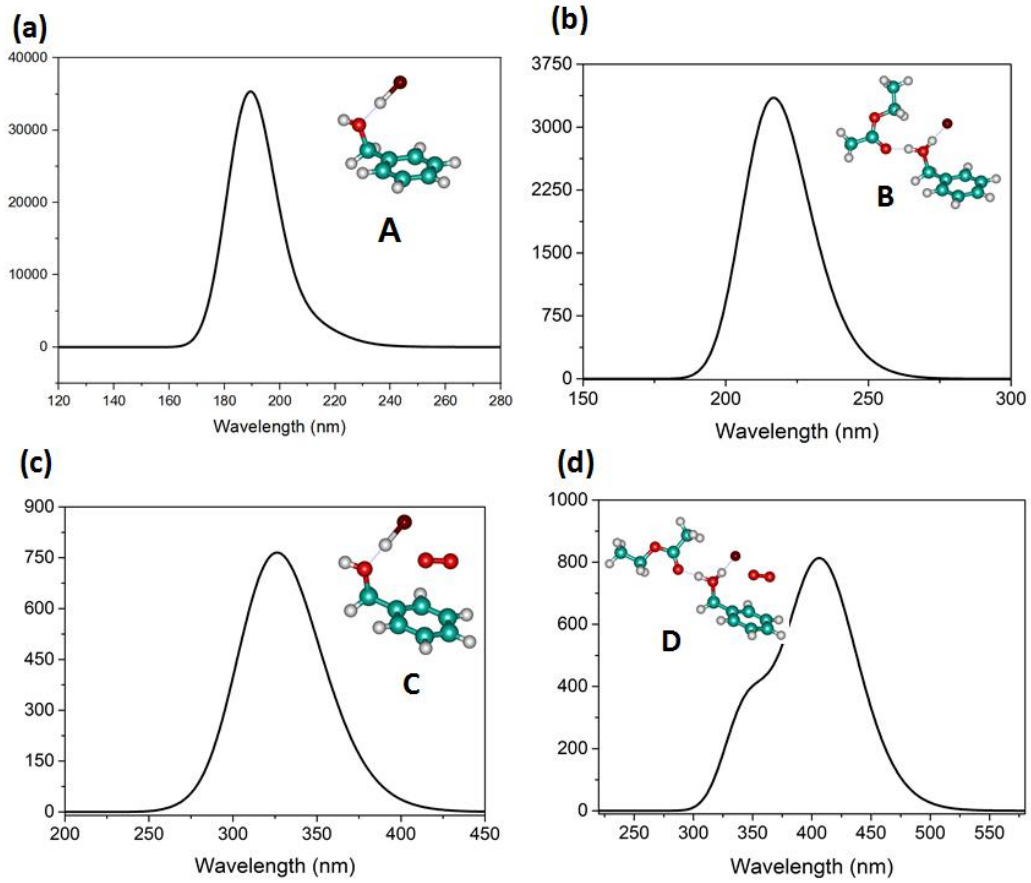

Figure S13. TD-DFT calculated absorption spectra for A, B, C and D structures.

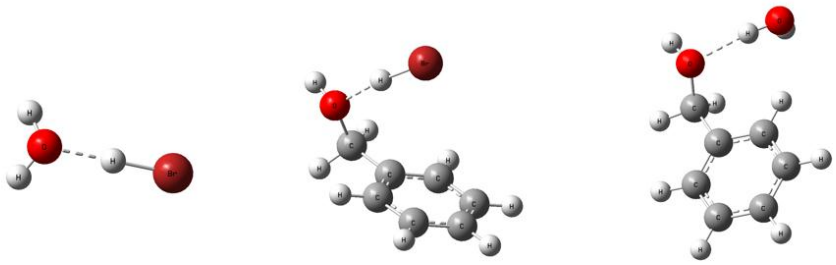

	H_2O-HBr	BnOH-HBr	BnOH-H_2O
H-Bond length (Å)	1.697	1.645	1.861
ρ_{BCP}	0.05023	0.05789	0.03284
BE (kcal/mol)	-10.46	-12.17	-6.58

Figure S14. Calculated hydrogen-bonding strengths, ρ_{BCP}, and binding energy (BE) of H_2O-HBr, BnOH-HBr, and BnOH-H_2O) complexes with the B3LYP/ma-TZVPP level.

We examined the hydrogen-bonding strengths for H_2O-HBr, BnOH-HBr, and BnOH-H_2O complexes. When H_2O and BnOH molecules both exist in the EtOAc solution, there is a competition for hydrogen bonding between HBr-H_2O and HBr-BnOH. In order to quantitatively clarify the hydrogen bonding energy, we utilized the method developed by Emamian *et al*.[12], which allows for accurate estimation of the binding energy (BE) of intermolecular hydrogen bonds through the below fitted equation based on high-level quantum chemical calculations (CCSD(T)/jul-cc-pVDZ + counterpoise):

$$BE/(kcal/mol) = -223.08*\rho_{BCP} + 0.7423$$

Where ρ_{BCP} is the electron density at bond critical point (hydrogen bond). Hence, we calculated the ρ_{BCP} for the three H-bonding structures (H_2O-HBr, BnOH-HBr, and BnOH-H_2O) by using Multiwfn package at the B3LYP/ma-TZVPP level of theory within the EtOAc solvation.

Table S2. Transition compositions, electronic excitation energy (nm), and the corresponding oscillator strengths for D complex based on TD-DFT method.

State	Transition	Contrib.	E (nm)	*f*
$T_0 \rightarrow T_1$	HOMO->LUMO	98.2%	411.5	0.0034
$T_0 \rightarrow T_2$	HOMO->LUMO+1	97.6%	408.2	0.0104

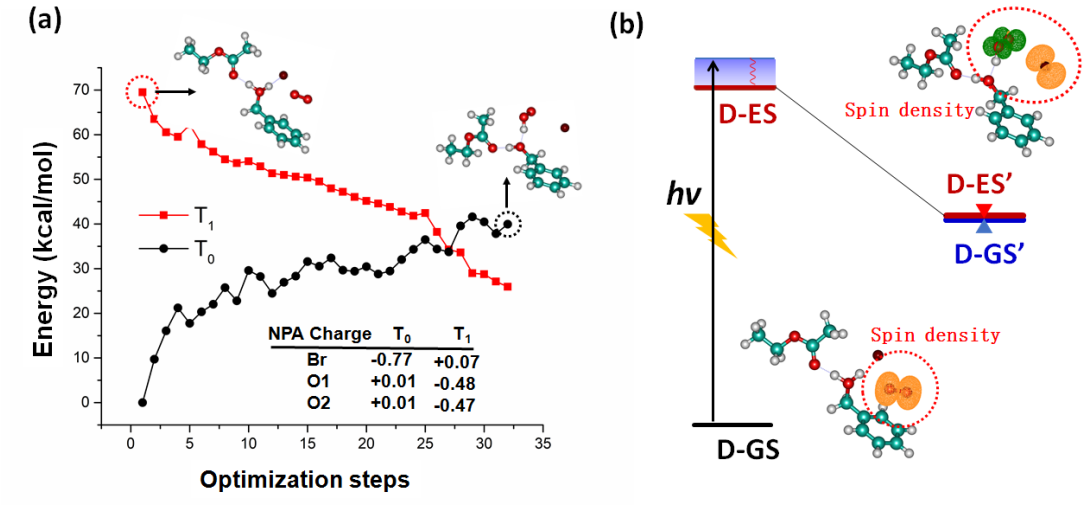

Figure S15. (a) Potential energy profile of ground state (T_0) and first excited state (T_1) of complex D in EtOAc through geometry relaxation on T_1 PES at SMD/CAM-B3LYP-D3/TZVP level of theory. (b) Schematic view for the photoexcitation and conical intersection process. The conical intersection geometry is denoted by D-ES' and D-GS'; spin densities for D-GS and D-GS' are calculated by the Multiwfn package with the isovalue set as 0.005; the molecular structure was depicted by VMD.[13]

The geometry relaxation for the EtOAc solvated **D** on T_1 potential energy surface (PES) was performed at the SMD/CAM-B3LYP-D3/TZVP level, as depicted in **Figure S15**. It shows that along structural optimization steps on T_1 PES, the O_2 group approaches to the hydroxyl-bonded proton and leads to the formation of OOH. **Figure S15(a)** reveals that there should be a conical intersection (CI) between T_1 and ground state along the relaxation process, which leads to the recovery of ground state populations via T_0-T_1 CI. The conical interaction structure (**D**-GS'/ES') was optimized using TD-DFT method at the same level of theory with the convergence on T_1/T_0 energy difference less than 0.0001 Hatree. Spin density analysis (**Figure S15(b)**) for ground state **D**-GS and CI structure was shown in **Figure S15(b**). It indicates that in ground state **D**-GS the spin densities locate on

the O_2 molecule, revealing that **D**-GS is a triplet state. For the CI geometry (**D**-GS'), both the OOH and Br group have unpaired electrons, showing a typical double radical state. For this double radical state, the system has energy-equivalent states with spin multiplicities of singlet or triplet. Since the final products are all in singlet states, we consider this state as an open-shell singlet state and carried out calculations for the reaction process on the open-shell singlet state.

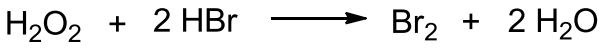

Figure S16 The equation of the reaction of H_2O_2 and HBr

In HBr system, the in situ generated H_2O_2 quickly reacts with HBr to produce H_2O and bromine.[14, 15] Since bromine is unstable in the presence of light, it decomposes to produce Br• radical under light irradiation,[16] which involves in the photo-induced alcohol oxidation in Scheme 1.

Spectral (^{1}H NMR & ^{13}C NMR) Data

The citation of reported product molecules provided with the the ^{1}H NMR, ^{13}C NMR, and HRMS data. As follow:

2a-2f ,[17] **2g-2h,** [18] **2i-2j**, [19] **2k**, [17] **2l**, [20] **2m**, [21] **2n**, [18] **2o**, [20] **2p**, [17] **2q**, [21] **2r**, [17] **2s**, [22] **2t**, [27] **2u**, [18] **2v,**[19] **2w,** [18] **2x-2,** [23] **2aa,** [27] **2ab,** [24] **2ac,** [25] **2ad,** [26] **2ae,** [27], **2af,** [19] **2ag,** [28] **2ah,** [19] **2ai-2al,** [27] **2am,**[19] **2an,** [27], **2ao,**[29] **2ap,** [28] **2aq.** [31]

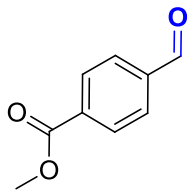

Compound **2o**: methyl 4-formylbenzoate

^{1}H NMR: (400 MHz, $CDCl_3$) δ 10.10 (s, 1H), 8.20 (d, J = 8.0 Hz, 1H), 7.95 (d, J = 8.0 Hz, 2H), 3.96 (s, 3H); ^{13}C NMR: (100 MHz, $CDCl_3$) δ 191.8, 166.2, 139.3, 135.3, 130.4, 129.8, 52.7.

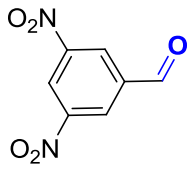

Compound **2s**: 3, 5-dinitrobenzaldehyde

^{1}H NMR: (400 MHz, $CDCl_3$) δ 10.22 (s, 1H), 9.28 (t, J = 2.0 Hz, 1H), 9.04 (d, J = 2.0 Hz, 1H); ^{13}C NMR: (100 MHz, $CDCl_3$) δ 187.2, 149.4, 138.7, 128.8, 123.4.

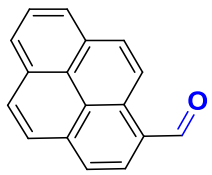

Compound **2w**: pyrene-1-carbaldehyde

^{1}H NMR: (400 MHz, $CDCl_3$) δ 10.74 (s, 1H), 9.36 (d, J = 8.8 Hz, 1H), 8.38 (d, J = 8.0 Hz, 1H), 8.28-8.25 (m, 3H), 8.20-8.17 (m, 2H), 8.08-8.03 (m, 2H); ^{13}C NMR: (100 MHz, $CDCl_3$) δ 193.2, 135.6, 131.4, 131.1, 131.0, 130.9, 130.8, 130.5, 127.5, 127.3, 127.1,126.9, 126.7, 124.7, 124.6, ,124.1, 123.1.

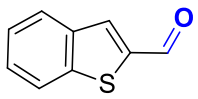

Compound **2y**: benzo[b]thiophene-2-carbaldehyde

^{1}H NMR: (400 MHz, $CDCl_3$) δ 10.11 (s, 1H), 8.03 (s, 1H), 7.91 (dd, J = 8.0 Hz, 8.0 Hz, 2H), 7.52 (t, J = 7.6 Hz, 1H), 7.45 (t, J = 7.6 Hz, 1H); ^{13}C NMR: (100 MHz, $CDCl_3$) δ 184.8, 143.5, 142.8, 138.7, 134.6, 128.3, 126.4, 125.4, 123.5.

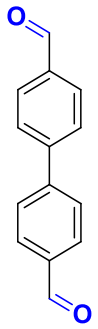

Compound **2ab**: [1,1'-biphenyl]-4,4'-dicarbaldehyde

^{1}H NMR: (400 MHz, $CDCl_3$) δ 10.09 (s, 2H), 7.99 (d, J = 8.0 Hz, 4.8 Hz, 4H), 7.80 (d, J = 4.8 Hz, 4H); ^{13}C NMR: (100 MHz, $CDCl_3$) δ 191.8, 145.7, 136.0, 130.5, 128.2.

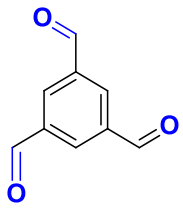

Compound **2ac**: benzene-1,3,5-tricarbaldehyde

^{1}H NMR: (400 MHz, $CDCl_3$) δ 10.20 (s, 3H), 8.64 (s, 3H); ^{13}C NMR: (100 MHz, $CDCl_3$) δ 190.0, 137.9, 134.9.

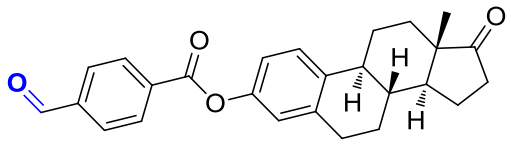

Compound **2ad**:

(8R,9S,13S,14S)-13-methyl-17-oxo-7,8,9,11,12,13,14,15,16,17-decahydro-6H-cyclopent a[a]phenanthren-3-yl 4-formylbenzoate

^{1}H NMR: (700 MHz, $CDCl_3$) δ 10.13 (s, 1H), 8.34 (d, J = 8.4 Hz, 2H), 8.01 (d, J = 8.4 Hz, 2H), 7.35 (d, J = 8.4 Hz, 1H), 7.00 (d, J = 8.4 Hz, 1H), 6.95 (d, J = 8.4 Hz, 1H), 2.94 (dd, J = 8.4 Hz, 2H), 2.51 (dd, J = 8.4 Hz, 1H), 2.45-2.41 (m, 1H), 2.34-2.30 (m, 1H), 2.18-2.11 (m, 1H), 2.09-2.02 (m, 2H), 1.99-1.97 (m, 1H), 1.67-1.61 (m, 2H), 1.59-1.46 (m, 4H), 0.92 (s, 3H); ^{13}C NMR: (150 MHz, $CDCl_3$) δ 191.7, 164.6, 148.7, 139.6, 138.4, 137.9, 134.7, 130.8, 129.7, 126.7, 121.6, 118.8, 50.5, 48.0, 44.3, 38.1, 36.0, 31.7, 29.8, 29.6, 26.4, 25.9, 21.7, 13.9.

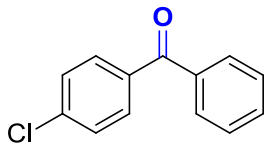

Compound **2af**: (4-chlorophenyl)(phenyl)methanone

^{1}H NMR: (400 MHz, $CDCl_3$) δ 7.76 (t, J = 6.8 Hz, 4H), 7.60 (t, J = 6.8 Hz, 1H), 7.44 (dd, J = 8.0 Hz, 7.6 Hz, 4H); ^{13}C NMR: (100 MHz, $CDCl_3$) δ 195.6, 139.0, 137.4, 136.0, 132.8, 131.6, 130.0, 128.8, 128.5.

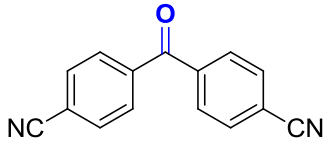

Compound **2ag**: 4,4'-carbonyldibenzonitrile

^{1}H NMR: (400 MHz, $CDCl_3$) δ 7.87 (d, J = 7.6 Hz, 4H), 7.82 (d, J = 7.6 Hz, 4H); ^{13}C NMR: (100 MHz, $CDCl_3$) δ 193.5, 139.8, 132.6, 130.3, 117.8, 116.6.

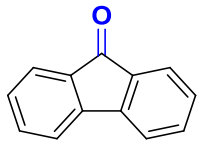

Compound **2ah**: 9H-fluoren-9-one

^{1}H NMR: (400 MHz, $CDCl_3$) δ 7.64 (d, J = 7.6 Hz, 2H), 7.50-7.44 (m, 4H), 7.29-7.25 (m, 2H); ^{13}C NMR: (100 MHz, $CDCl_3$) δ 194.0, 144.5, 134.8, 134.2, 129.1, 124.4, 120.4.

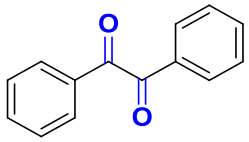

Compound **2ai**: benzophenone

^{1}H NMR: (400 MHz, $CDCl_3$) δ 7.98 (d, J = 7.6 Hz, 4H), 7.66 (t, J = 7.6 Hz, 2H), 7.51 (t, J = 7.6Hz, 4H); ^{13}C NMR: (100 MHz, $CDCl_3$) δ 194.7, 135.0, 133.1, 130.0, 129.2.

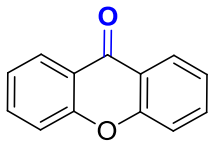

Compound **2ak**: 9H-xanthen-9-one

^{1}H NMR: (400 MHz, $CDCl_3$) δ 8.33 (dd, J = 8.0 Hz, 8.0 Hz, 2H), 7.73-7.69 (m, 2H), 7.48 (d, J = 7.6 Hz, 2H), 7.39-7.35 (m, 2H),; ^{13}C NMR: (100 MHz, $CDCl_3$) δ 177.4, 156.3, 134.9, 126.9, 124.0, 122.0, 118.1;

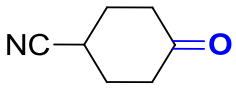

Compound **2ao**: 4-oxocyclohexanecarbonitrile

^{1}H NMR: (400 MHz, $CDCl_3$) δ 3.03-2.98 (m, 1H), 2.59-2.52 (m, 2H), 2.41-2.34 (m, 2H), 2.21-2.09 (m, 4H); ^{13}C NMR: (100 MHz, $CDCl_3$) δ 207.3, 120.6, 38.6, 29.1, 26.4.

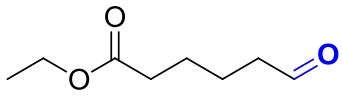

Compound **2aq**: ethyl 6-oxohexanoate

^{1}H NMR: (400 MHz, $CDCl_3$) δ 9.73 (1H), 4.09 (q, J = 7.2 Hz, 2H), 2.45-2.41 (m, 2H), 2.31-2.27 (m, 2H), 1.65-1.61 (m, 4H), 1.22 (t, J = 7.2 Hz, 3H); ^{13}C NMR: (100 MHz, $CDCl_3$) δ 202.2, 173.3, 60.4, 3.6, 34.0, 24.4, 21.6, 14.3.

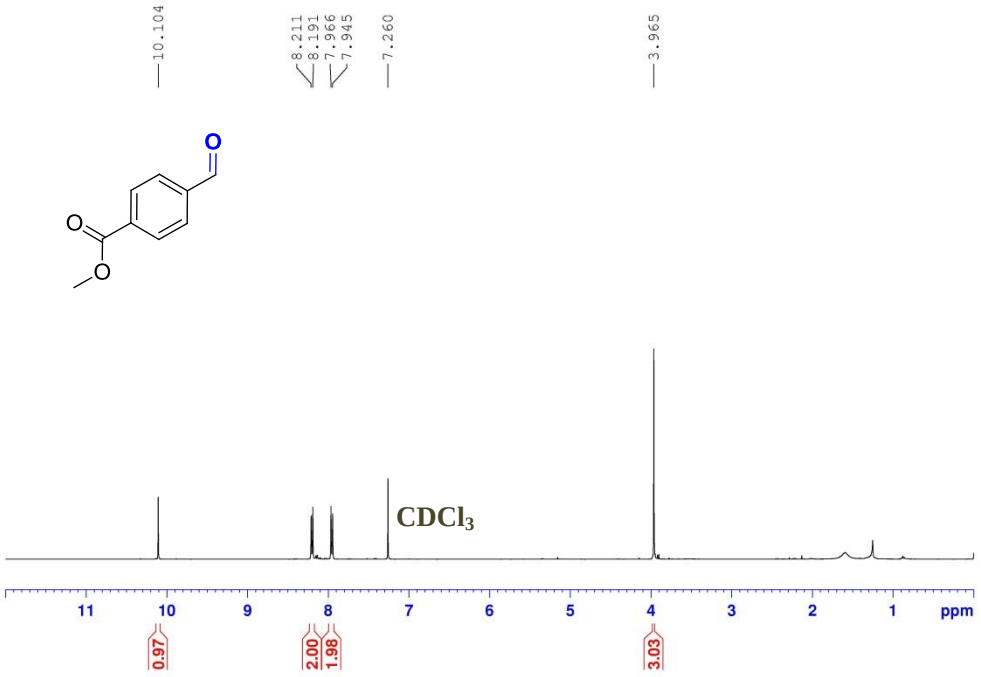
10.104
8.211
8.191
7.966
7.945
7.260
3.965
O
O
O
CDCl3
11
10
9
8
7
6
5
4
3
2
1
ppm
0.97
2.00
1.98
3.03

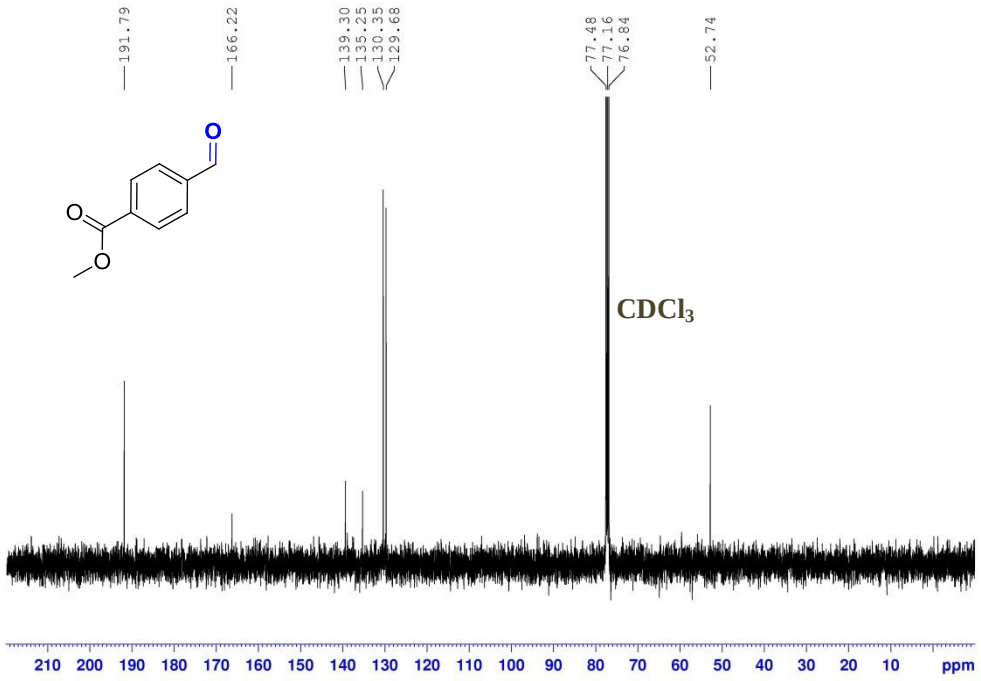
191.79
166.22
139.30
135.25
130.35
129.68
77.48
77.16
76.84
52.74
O
O
O
CDCl3
210
200
190
180
170
160
150
140
130
120
110
100
90
80
70
60
50
40
30
20
10
ppm

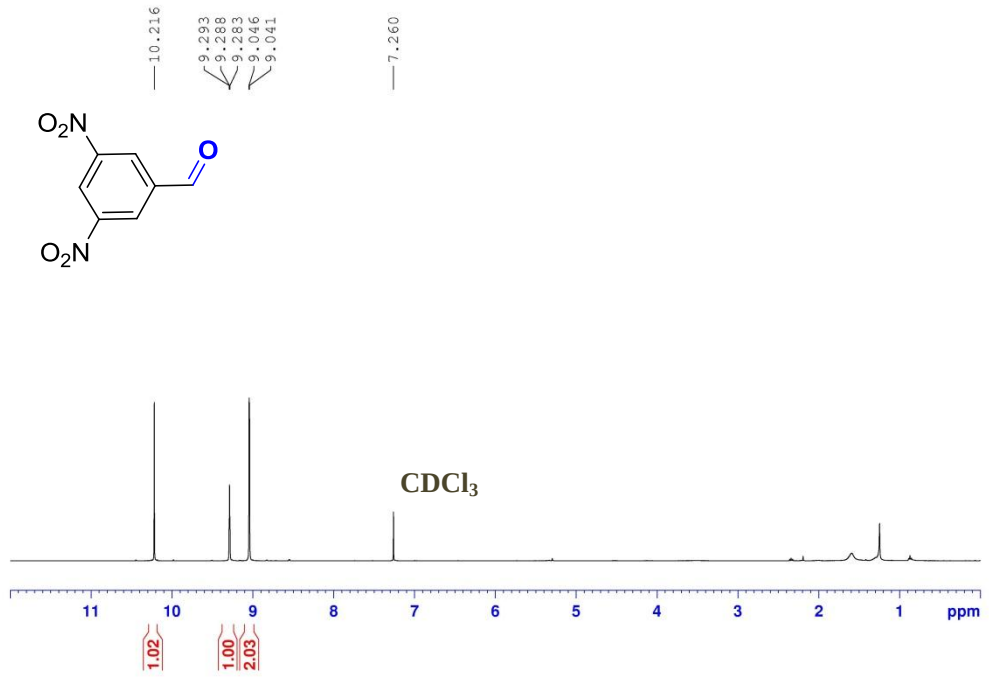
10.216
9.293
9.288
9.283
9.046
9.041
7.260
O2N
O
O2N
CDCl3
11
10
9
8
7
6
5
4
3
2
1
ppm
1.02
1.00
2.03

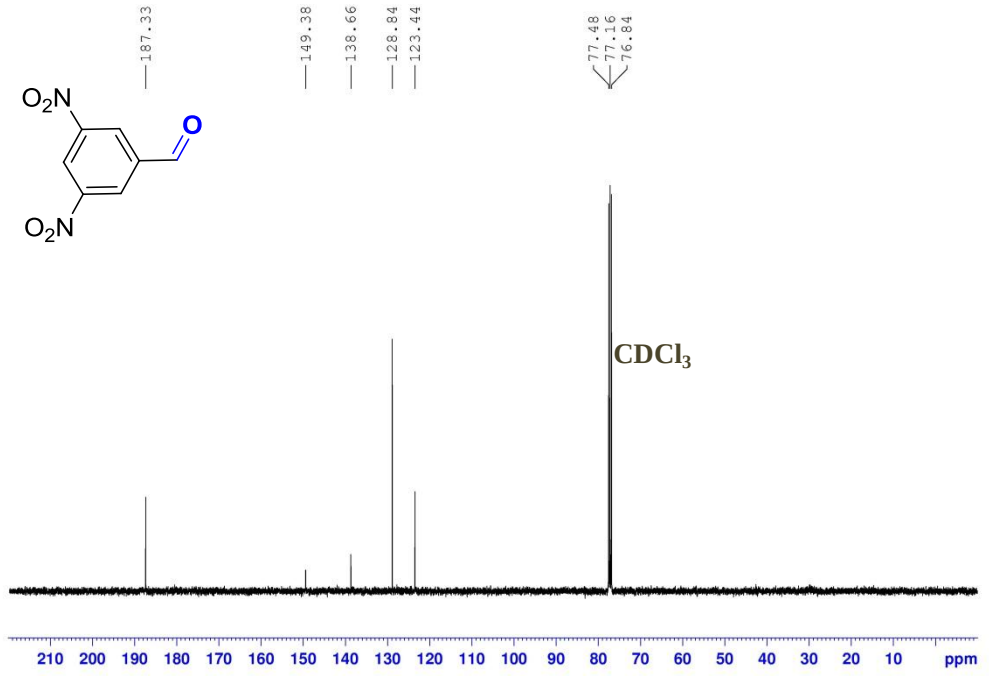
187.33
149.38
138.66
128.84
123.44
77.48
77.16
76.84
O2N
O
O2N
CDCl3
210
200
190
180
170
160
150
140
130
120
110
100
90
80
70
60
50
40
30
20
10
ppm

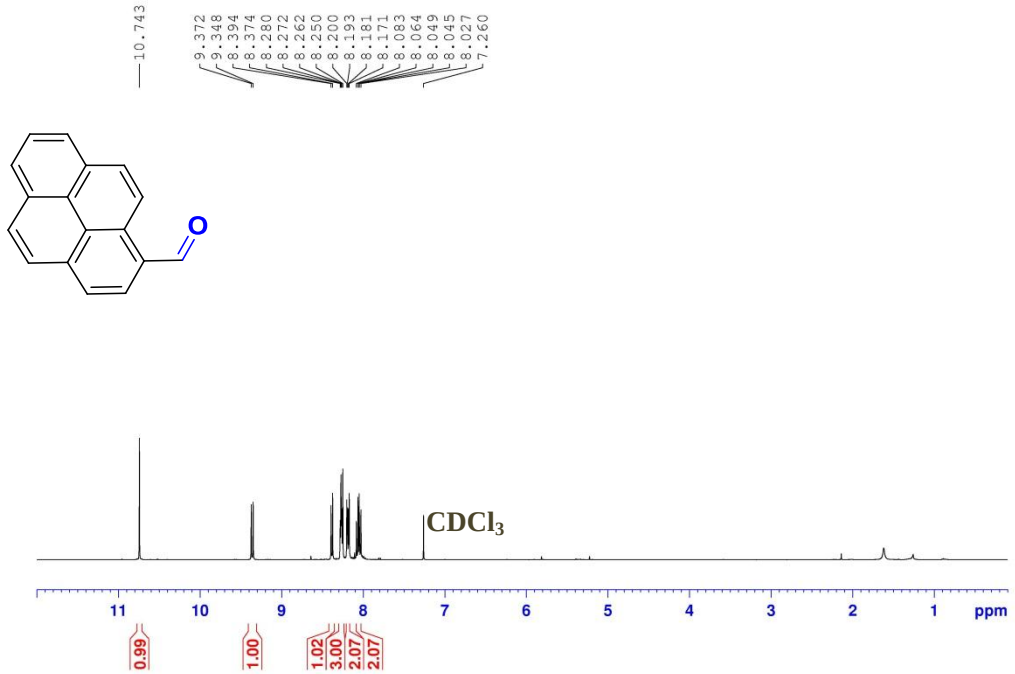
10.743
9.372
9.348
8.394
8.374
8.280
8.272
8.262
8.250
8.200
8.193
8.181
8.171
8.083
8.064
8.049
8.045
8.027
7.260
O
CDCl3
11
10
9
8
7
6
5
4
3
2
1
ppm
0.99
1.00
1.02
3.00
2.07
2.07

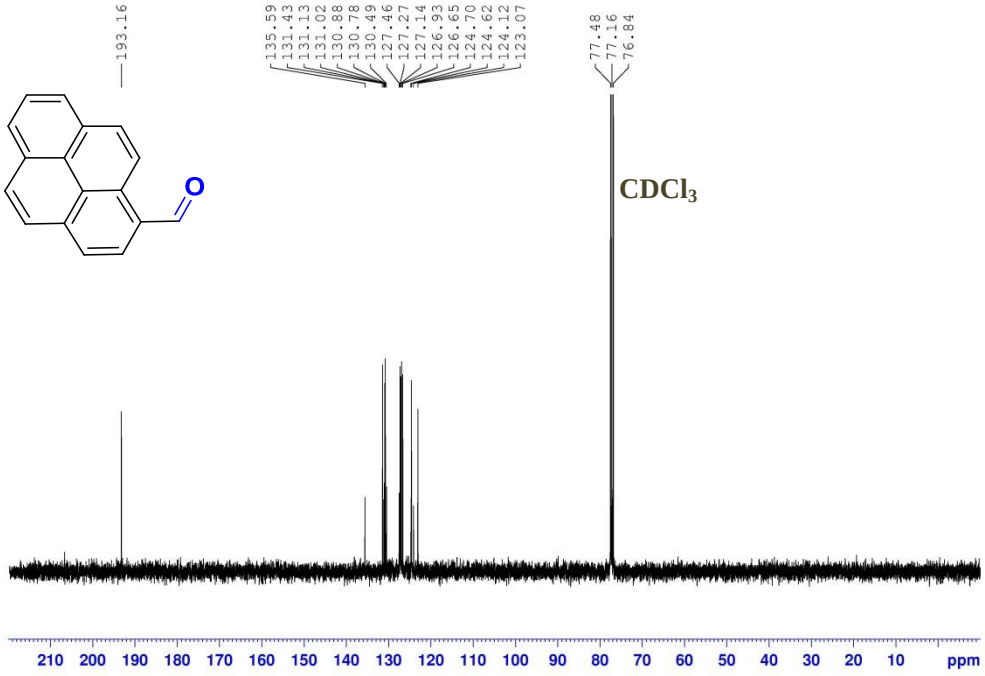
193.16
135.59
131.43
131.13
131.02
130.88
130.78
130.49
127.46
127.27
127.14
126.93
126.65
124.70
124.62
124.12
123.07
77.48
77.16
76.84
O
CDCl3
210
200
190
180
170
160
150
140
130
120
110
100
90
80
70
60
50
40
30
20
10
ppm

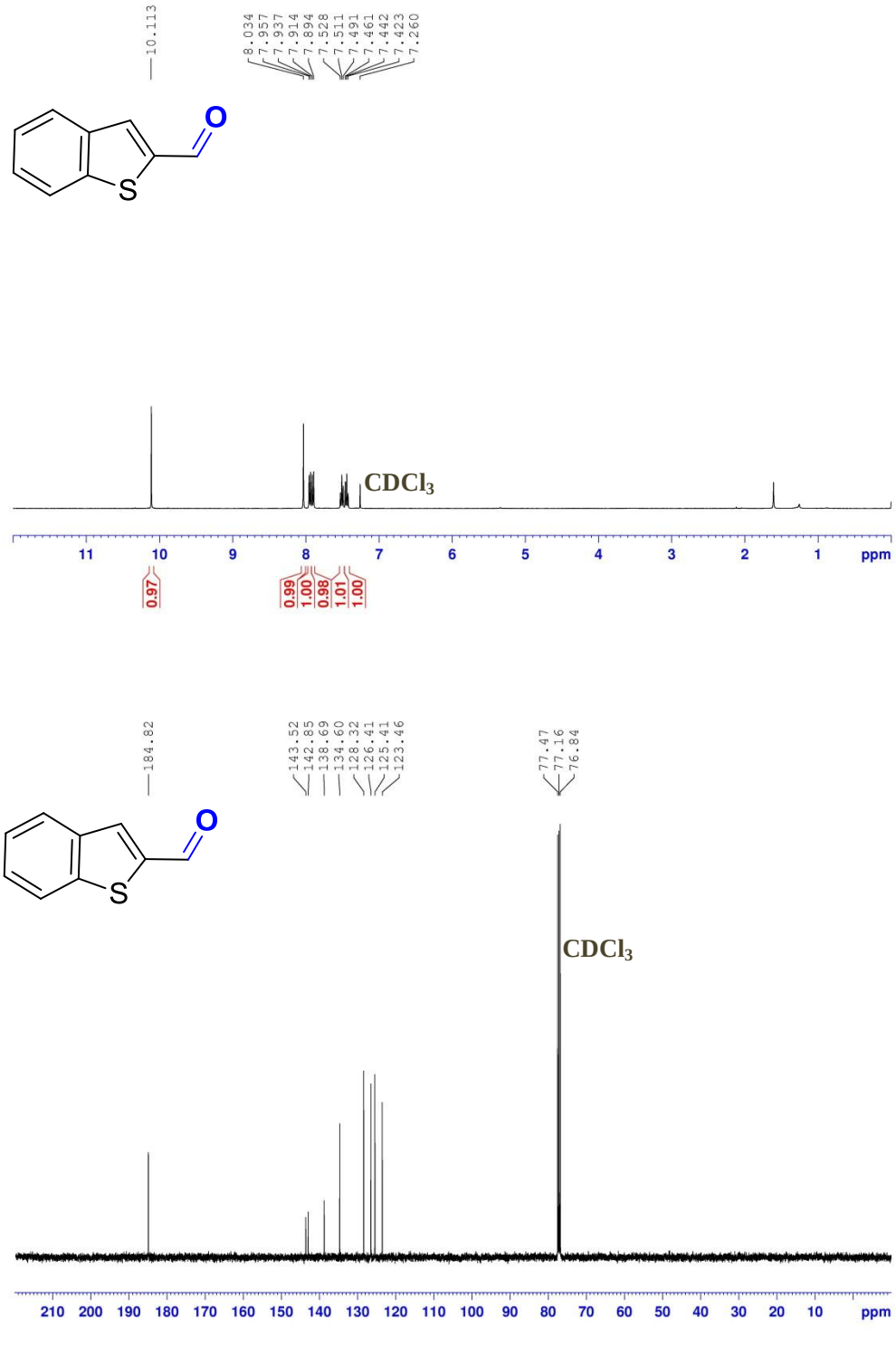
10.113
8.034
7.957
7.937
7.914
7.894
7.528
7.511
7.491
7.461
7.442
7.423
7.260
O
S
CDCl3
11
10
9
8
7
6
5
4
3
2
1
ppm
0.97
0.99
1.00
0.98
1.01
1.00
184.82
143.52
142.85
138.69
134.60
128.32
126.41
125.41
123.46
77.47
77.16
76.84
O
S
CDCl3
210
200
190
180
170
160
150
140
130
120
110
100
90
80
70
60
50
40
30
20
10
ppm

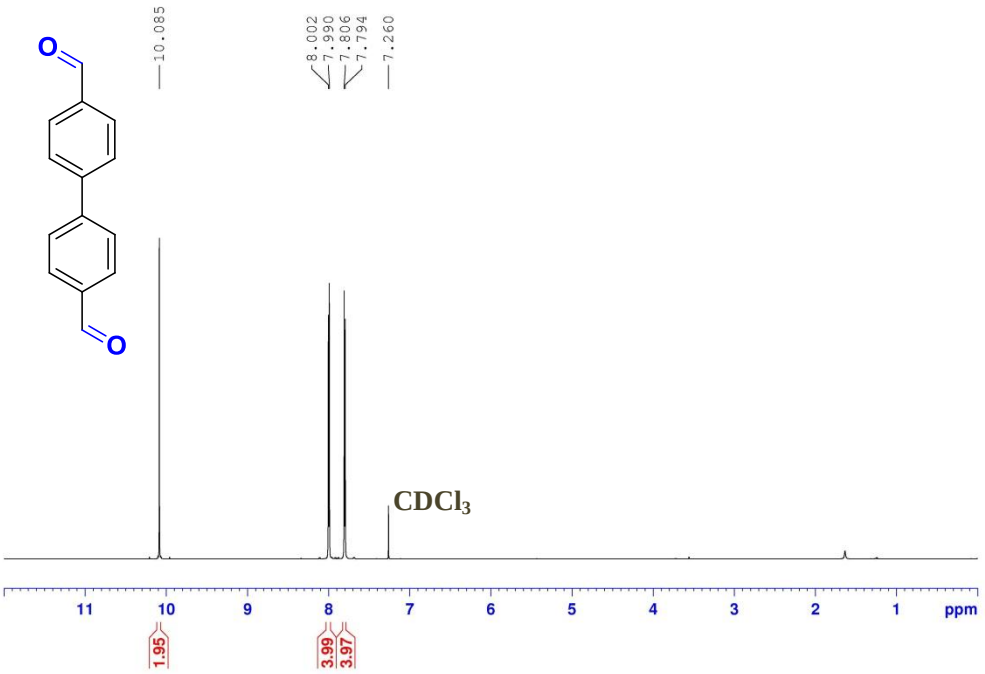
10.085
8.002
7.990
7.806
7.794
7.260
CDCl3
11
10
9
8
7
6
5
4
3
2
1
ppm
1.95
3.99
3.97

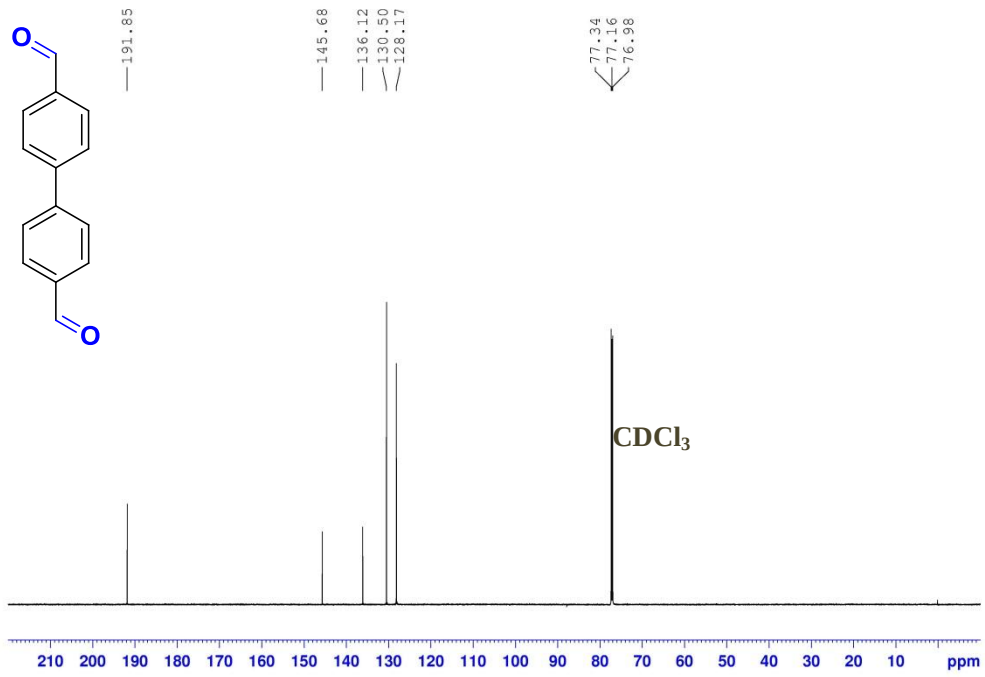
191.85
145.68
136.12
130.50
128.17
77.34
77.16
76.98
CDCl3
210
200
190
180
170
160
150
140
130
120
110
100
90
80
70
60
50
40
30
20
10
ppm

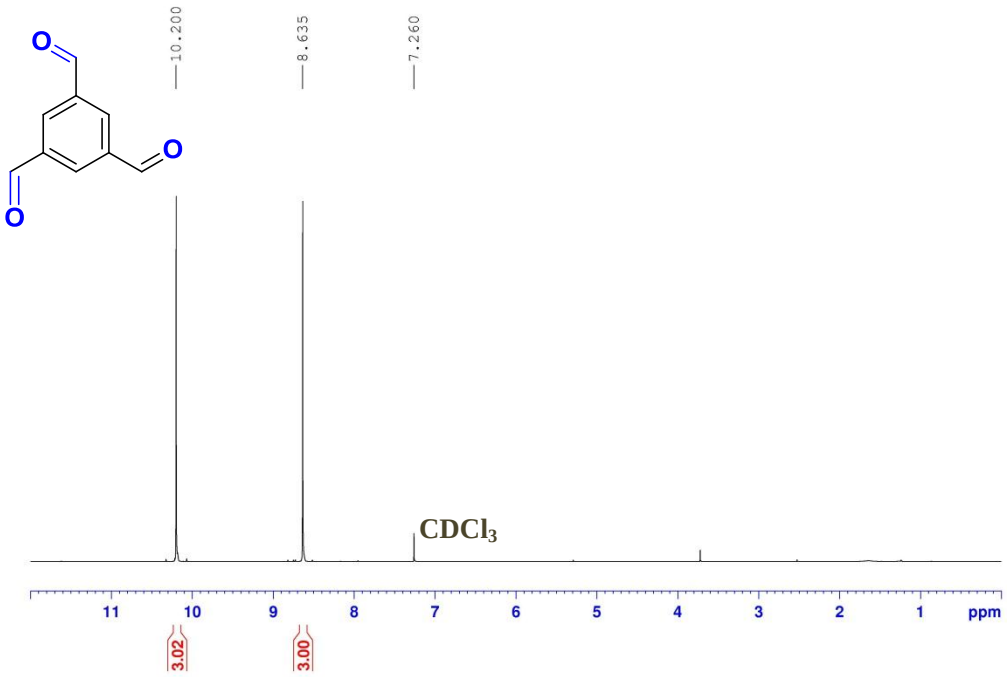
10.200
8.635
7.260
CDCl3
11
10
9
8
7
6
5
4
3
2
1
ppm
3.02
3.00

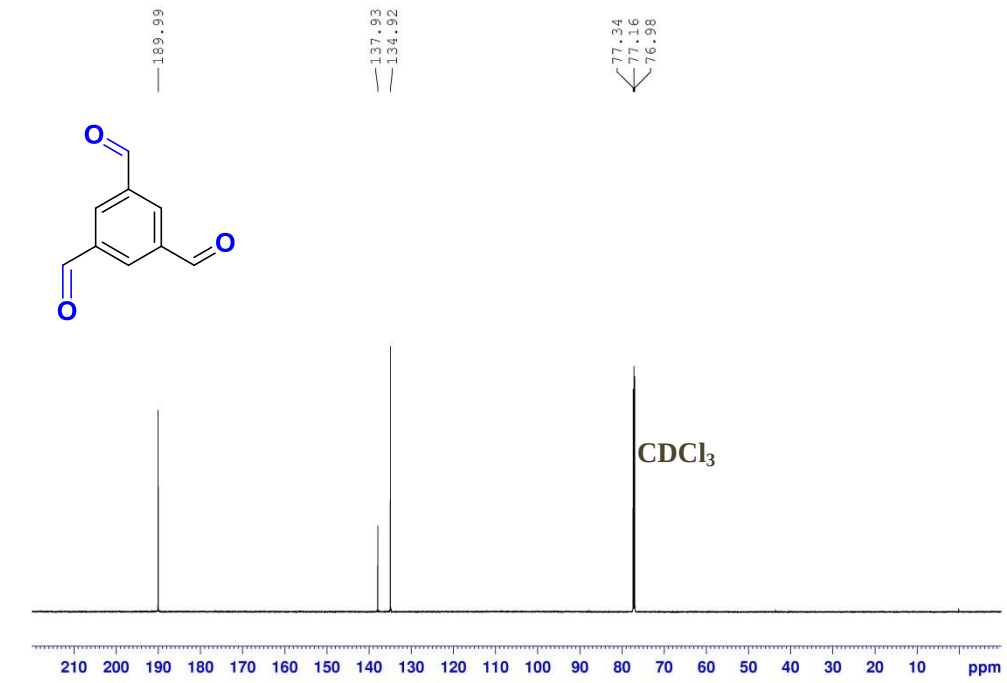
189.99
137.93
134.92
77.34
77.16
76.98
CDCl3
210
200
190
180
170
160
150
140
130
120
110
100
90
80
70
60
50
40
30
20
10
ppm

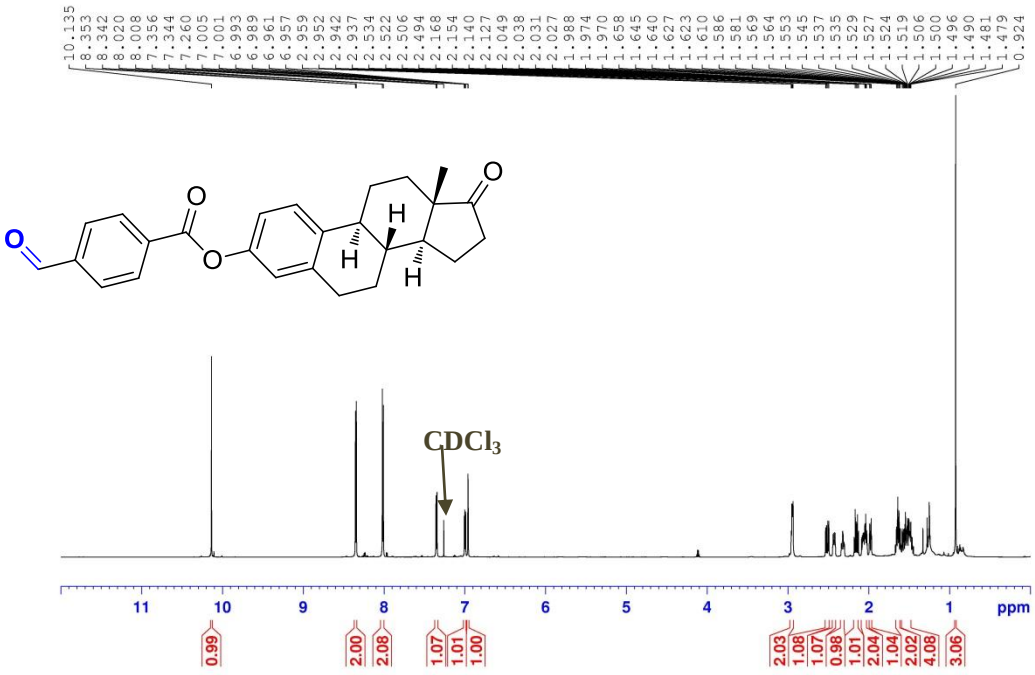
10.135
8.353
8.342
8.020
8.008
7.356
7.344
7.260
7.005
7.001
6.993
6.989
6.961
6.957
2.959
2.952
2.942
2.937
2.534
2.522
2.506
2.494
2.168
2.154
2.140
2.127
2.049
2.038
2.031
2.027
1.988
1.974
1.970
1.658
1.645
1.640
1.627
1.623
1.610
1.586
1.581
1.569
1.564
1.553
1.545
1.537
1.535
1.529
1.527
1.524
1.519
1.506
1.500
1.496
1.490
1.481
1.479
0.924
O
O
O
H
H
H
CDCl3
11
10
9
8
7
6
5
4
3
2
1
ppm
0.99
2.00
2.08
1.07
1.01
1.00
2.03
1.08
1.07
0.98
1.01
2.04
1.04
2.02
4.08
3.06

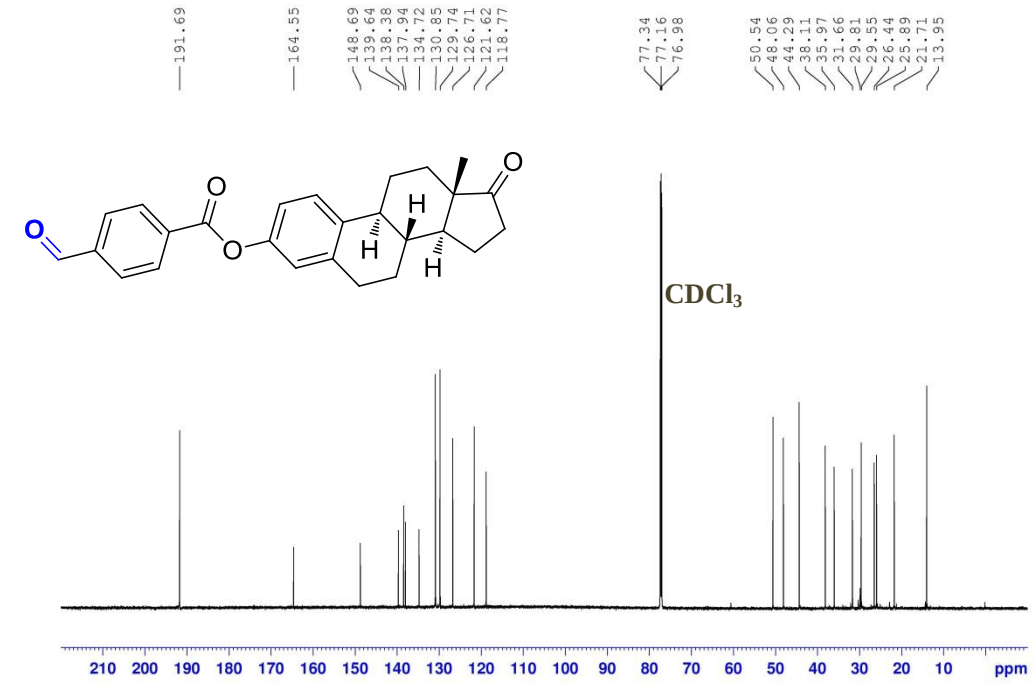
191.69
164.55
148.69
139.64
138.38
137.94
134.72
130.85
129.74
126.71
121.62
118.77
77.34
77.16
76.98
50.54
48.06
44.29
38.11
35.97
31.66
29.81
29.55
26.44
25.89
21.71
13.95
O
O
O
H
H
H
CDCl3
210
200
190
180
170
160
150
140
130
120
110
100
90
80
70
60
50
40
30
20
10
ppm

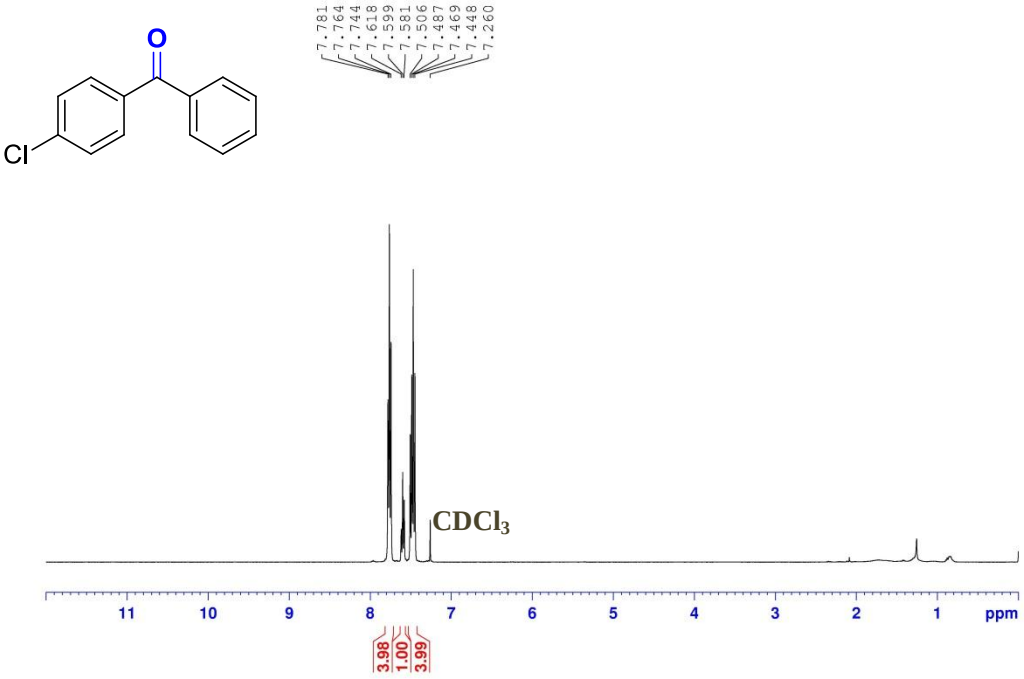
O
Cl
7.781
7.764
7.744
7.618
7.599
7.581
7.506
7.487
7.469
7.448
7.260
CDCl3
11
10
9
8
7
6
5
4
3
2
1
ppm
3.98
1.00
3.99

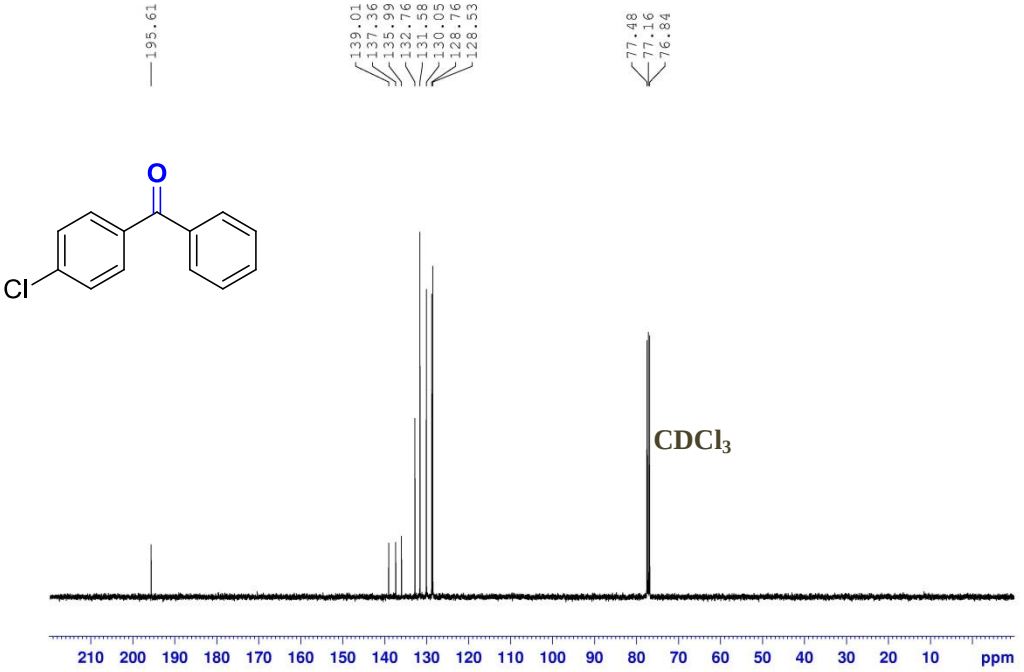
195.61
139.01
137.36
135.99
132.76
131.58
130.05
128.76
128.53
77.48
77.16
76.84
O
Cl
CDCl3
210
200
190
180
170
160
150
140
130
120
110
100
90
80
70
60
50
40
30
20
10
ppm

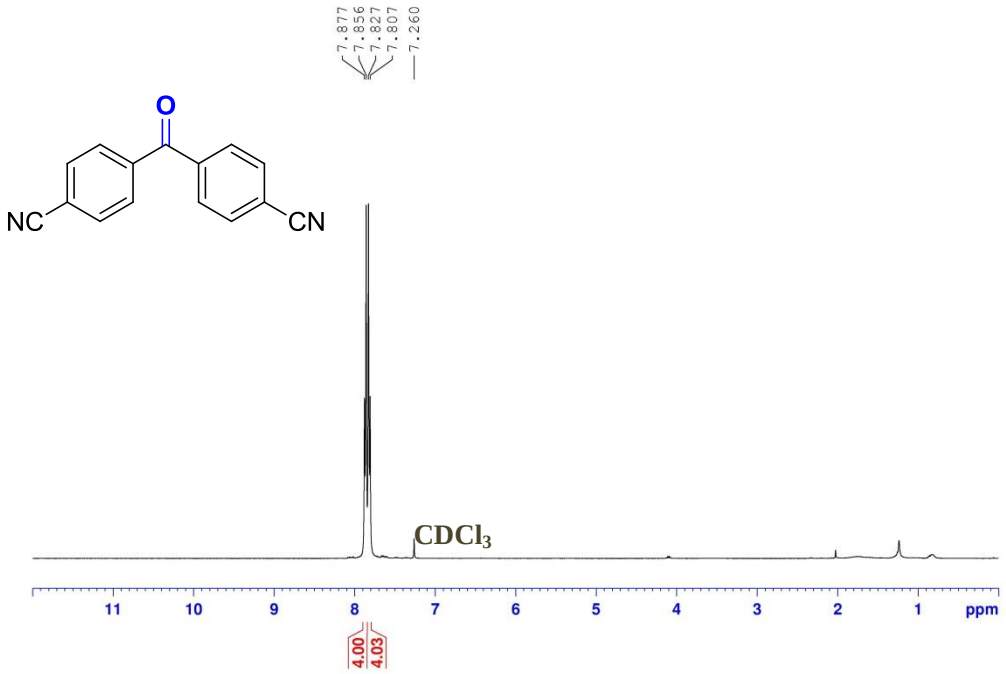
7.877
7.856
7.827
7.807
7.260
O
NC
CN
CDCl3
11
10
9
8
7
6
5
4
3
2
1
ppm
4.00
4.03

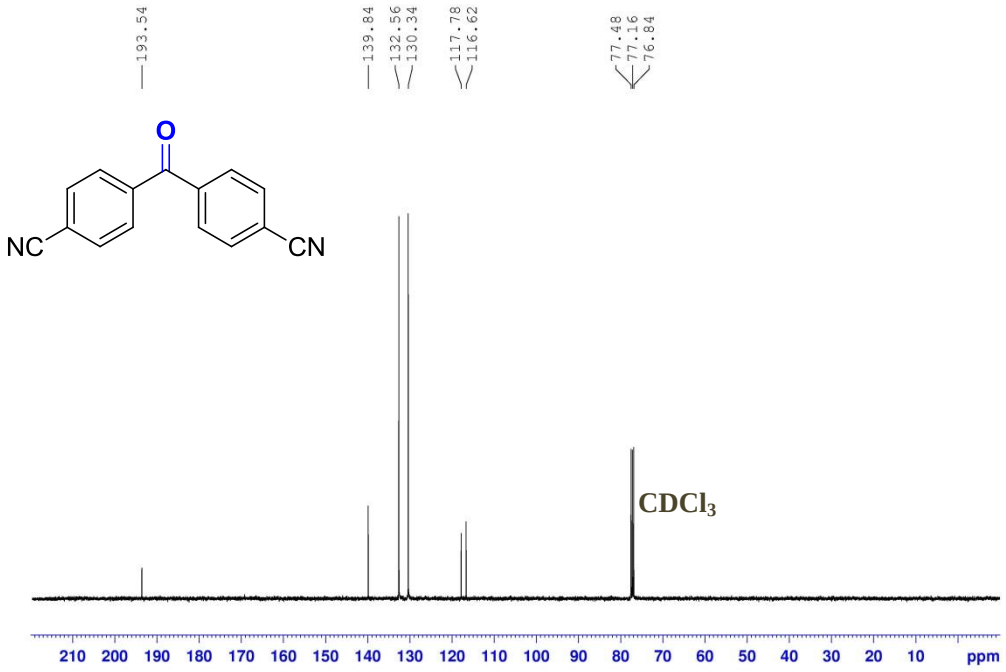
193.54
139.84
132.56
130.34
117.78
116.62
77.48
77.16
76.84
O
NC
CN
CDCl3
210
200
190
180
170
160
150
140
130
120
110
100
90
80
70
60
50
40
30
20
10
ppm

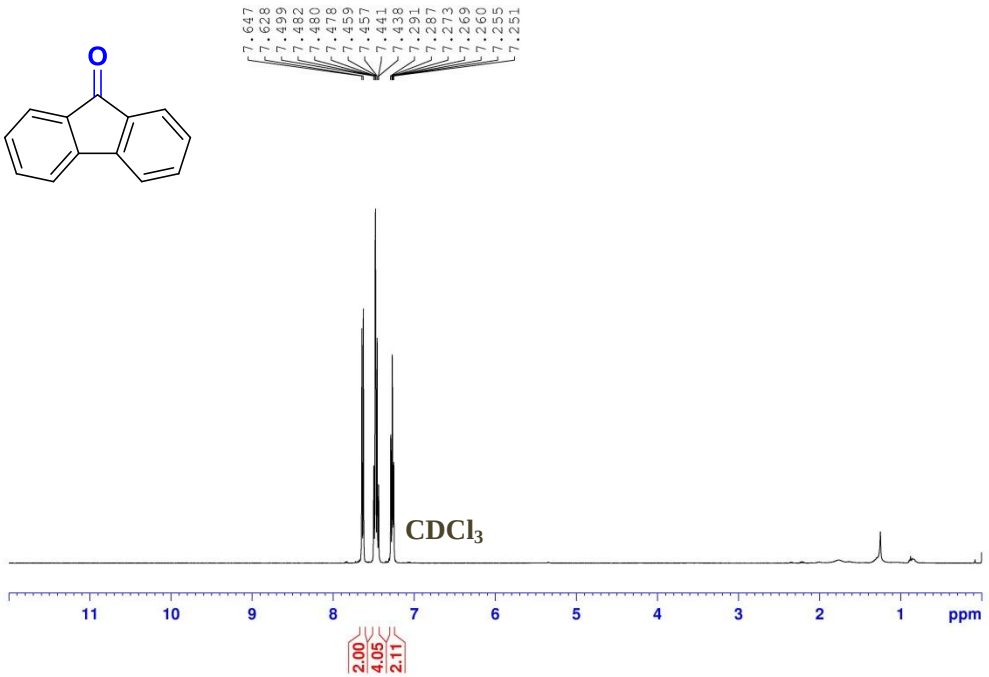
7.647
7.628
7.499
7.482
7.480
7.478
7.459
7.457
7.441
7.438
7.291
7.287
7.273
7.269
7.260
7.255
7.251
O
CDCl3
11
10
9
8
7
6
5
4
3
2
1
ppm
2.00
4.05
2.11

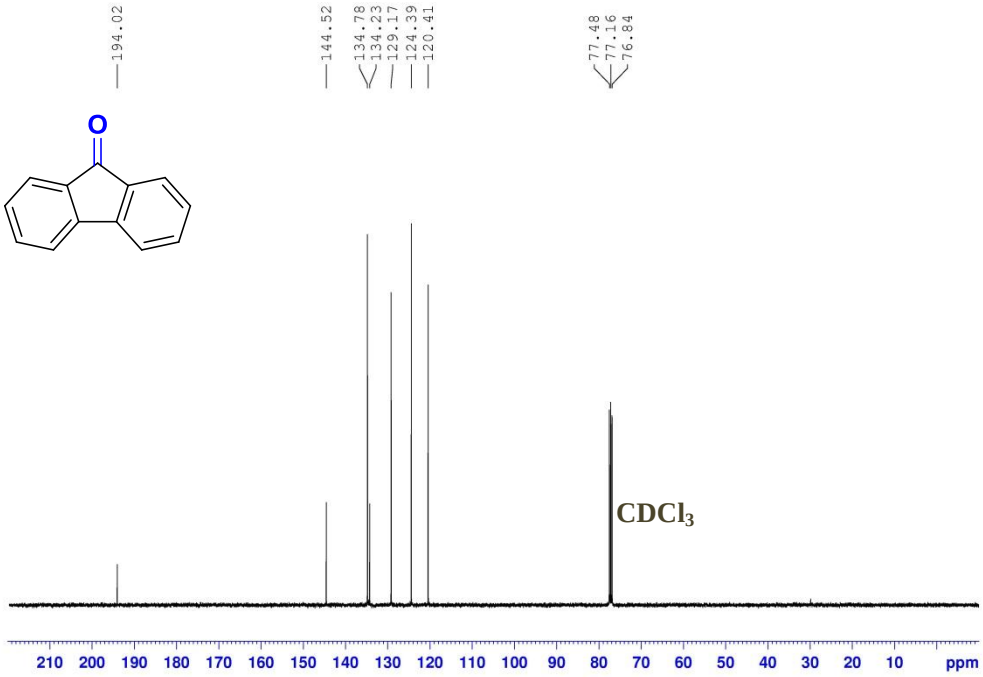
194.02
144.52
134.78
134.23
129.17
124.39
120.41
77.48
77.16
76.84
O
CDCl3
210
200
190
180
170
160
150
140
130
120
110
100
90
80
70
60
50
40
30
20
10
ppm

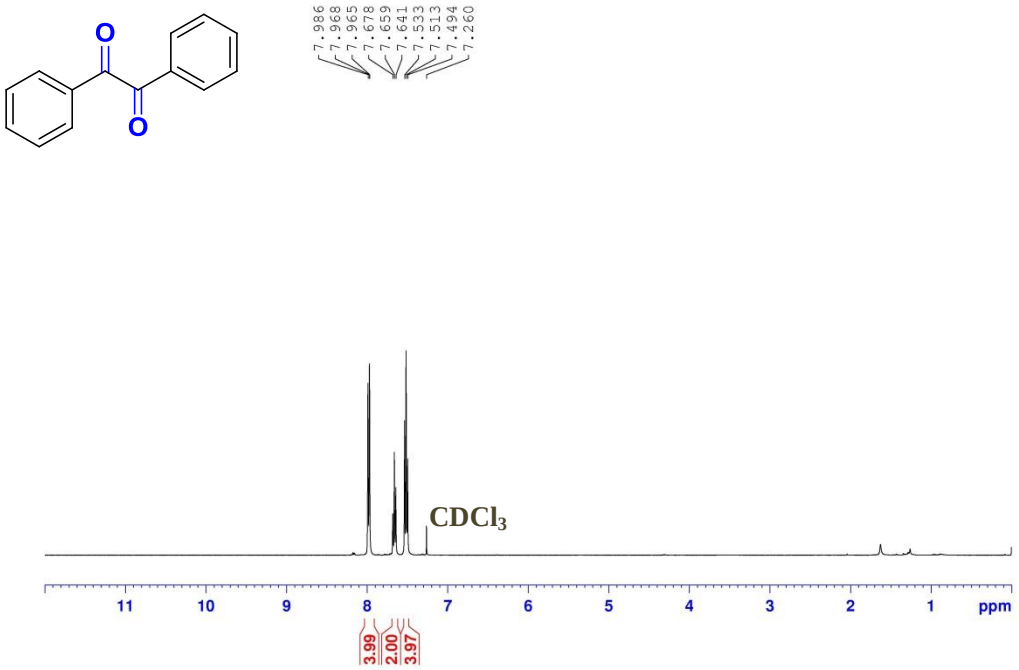
7.986
7.968
7.965
7.678
7.659
7.641
7.533
7.513
7.494
7.260
CDCl3
11
10
9
8
7
6
5
4
3
2
1
ppm
3.99
2.00
3.97

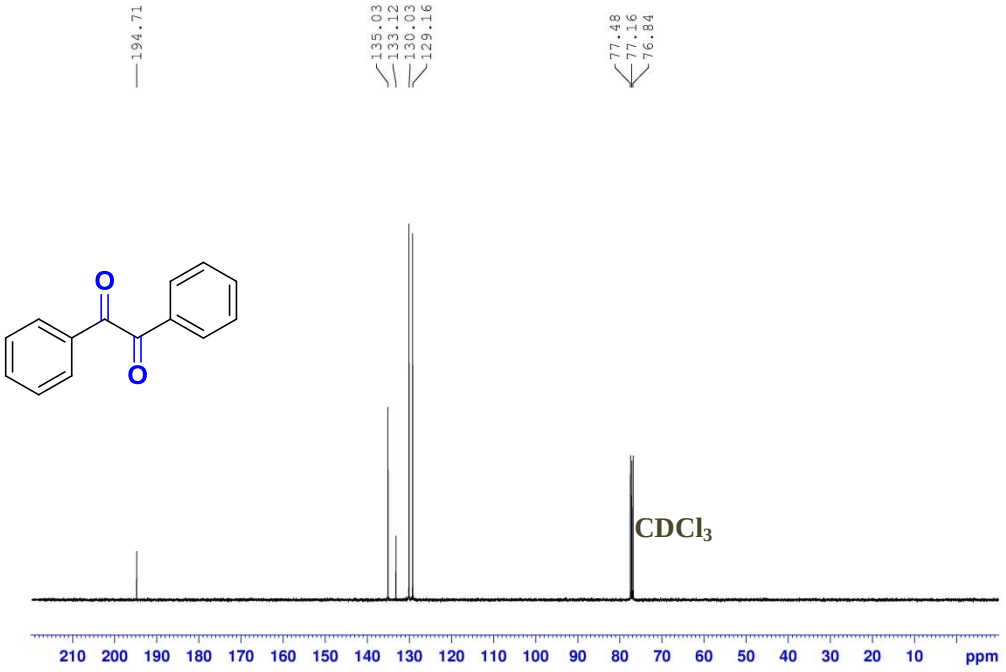
194.71
135.03
133.12
130.03
129.16
77.48
77.16
76.84
CDCl3
210
200
190
180
170
160
150
140
130
120
110
100
90
80
70
60
50
40
30
20
10
ppm

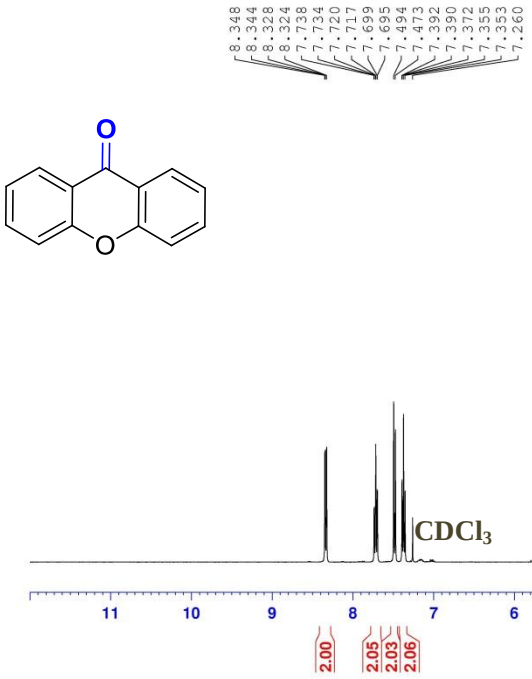
8.348
8.344
8.328
8.324
7.738
7.734
7.720
7.717
7.699
7.695
7.494
7.473
7.392
7.390
7.372
7.355
7.353
7.260
O
O
CDCl3
11
10
9
8
7
6
5
4
3
2
1
ppm
2.00
2.05
2.03
2.06

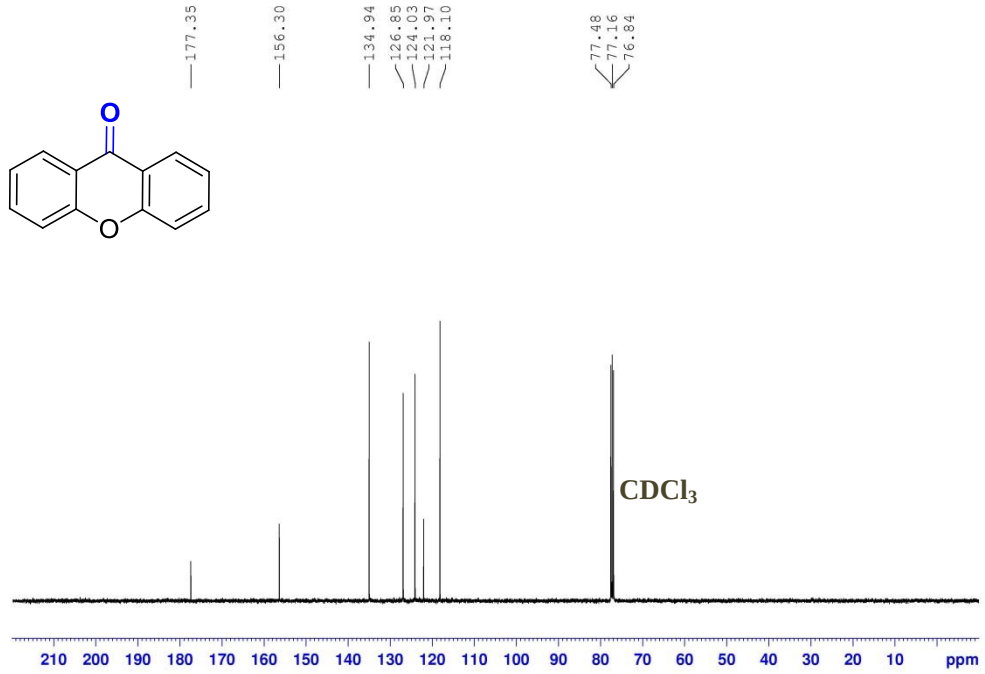
177.35
156.30
134.94
126.85
124.03
121.97
118.10
77.48
77.16
76.84
O
O
CDCl3
210
200
190
180
170
160
150
140
130
120
110
100
90
80
70
60
50
40
30
20
10
ppm

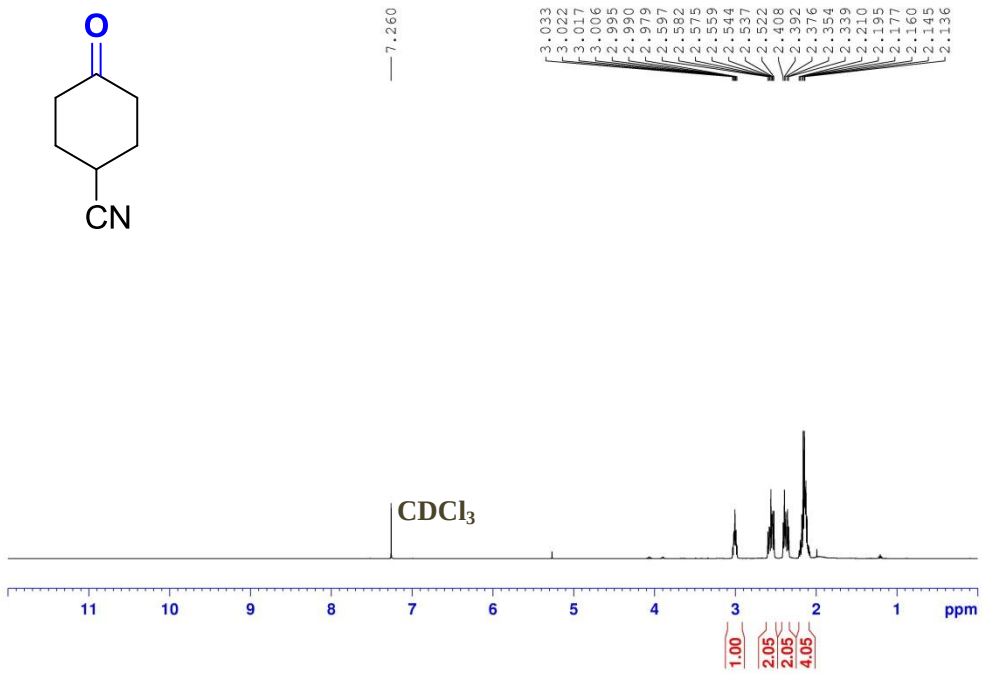
O
CN
7.260
3.033
3.022
3.017
3.006
2.995
2.990
2.979
2.597
2.582
2.575
2.559
2.544
2.537
2.522
2.408
2.392
2.376
2.354
2.339
2.210
2.195
2.177
2.160
2.145
2.136
CDCl3
11
10
9
8
7
6
5
4
3
2
1
ppm
1.00
2.05
2.05
4.05

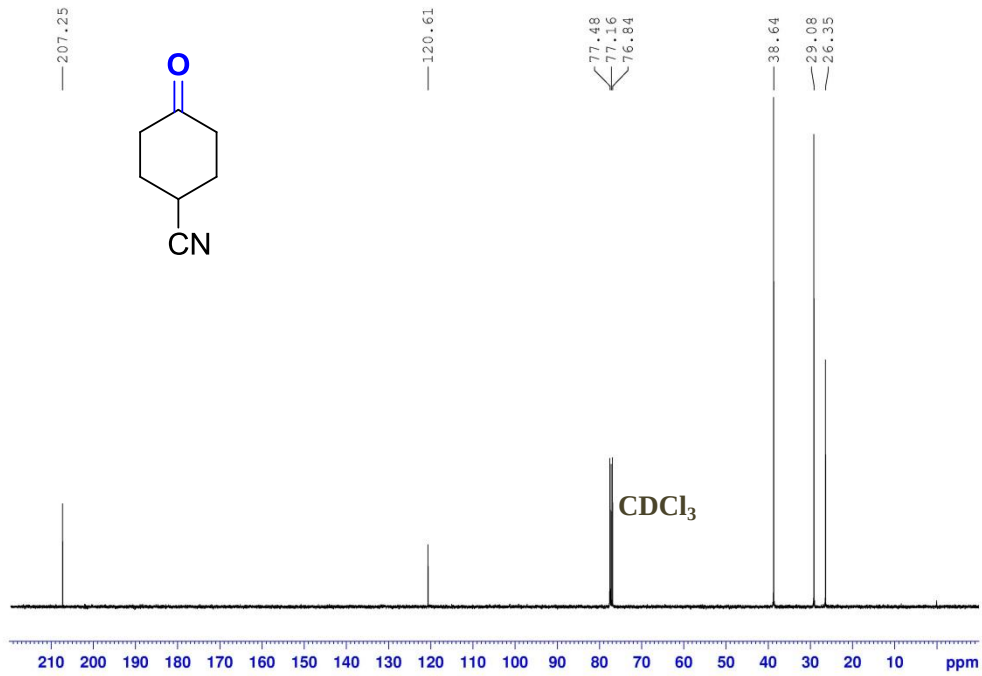
207.25
120.61
77.48
77.16
76.84
38.64
29.08
26.35
O
CN
CDCl3
210
200
190
180
170
160
150
140
130
120
110
100
90
80
70
60
50
40
30
20
10
ppm

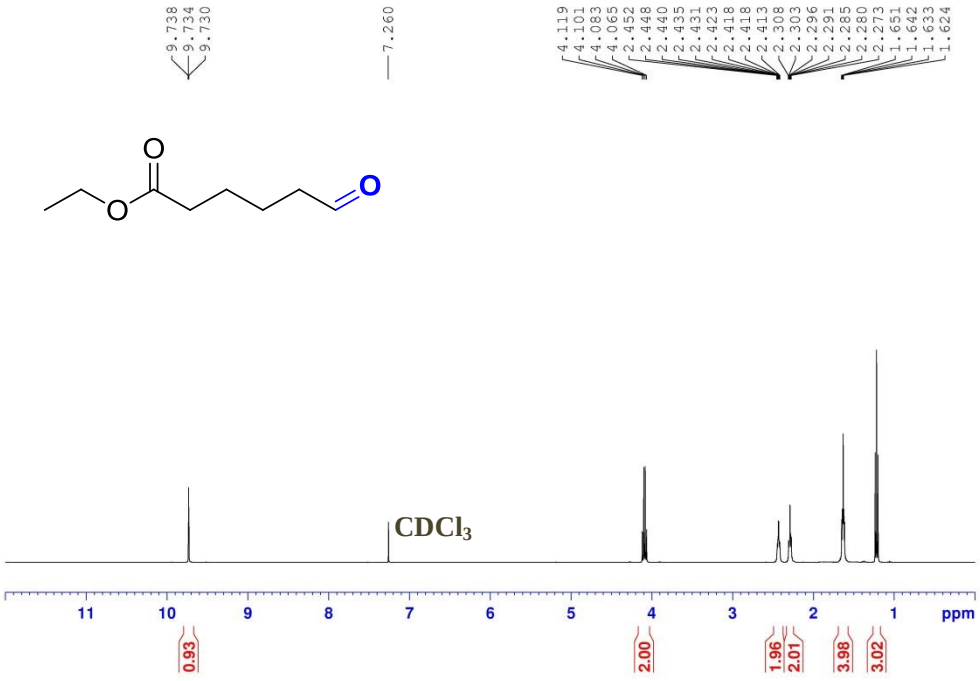
9.738
9.734
9.730
7.260
4.119
4.101
4.083
4.065
2.452
2.448
2.440
2.435
2.431
2.423
2.418
2.413
2.308
2.303
2.296
2.291
2.285
2.280
2.273
1.651
1.642
1.633
1.624
O
O
O
CDCl3
11
10
9
8
7
6
5
4
3
2
1
ppm
0.93
2.00
1.96
2.01
3.98
3.02

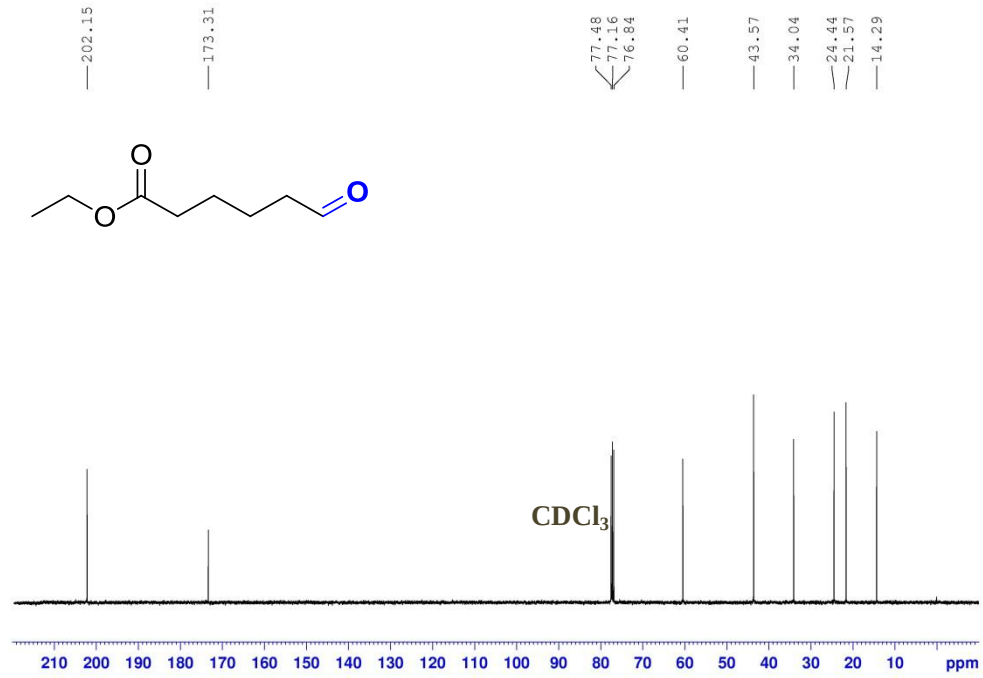
202.15
173.31
77.48
77.16
76.84
60.41
43.57
34.04
24.44
21.57
14.29
O
O
O
CDCl3
210
200
190
180
170
160
150
140
130
120
110
100
90
80
70
60
50
40
30
20
10
ppm

References

1. M. J. Frisch, G. W. Trucks, H. B. Schlegel, G. E. Scuseria, M. A. Robb, J. R. Cheeseman, G. Scalmani, V. Barone, G. A. Petersson, H. Nakatsuji, X. Li, M. Caricato, A. V. Marenich, J. Bloino, B. G. Janesko, R. Gomperts, B. Mennucci, H. P. Hratchian, J. V. Ortiz, A. F. Izmaylov, J. L. Sonnenberg, Williams, F. Ding, F. Lipparini, F. Egidi, J. Goings, B. Peng, A. Petrone, T. Henderson, D. Ranasinghe, V. G. Zakrzewski, J. Gao, N. Rega, G. Zheng, W. Liang, M. Hada, M. Ehara, K. Toyota, R. Fukuda, J. Hasegawa, M. Ishida, T. Nakajima, Y. Honda, O. Kitao, H. Nakai, T. Vreven, K. Throssell, J. A. Montgomery Jr., J. E. Peralta, F. Ogliaro, M. J. Bearpark, J. J. Heyd, E. N. Brothers, K. N. Kudin, V. N. Staroverov, T. A. Keith, R. Kobayashi, J. Normand, K. Raghavachari, A. P. Rendell, J. C. Burant, S. S. Iyengar, J. Tomasi, M. Cossi, J. M. Millam, M. Klene, C. Adamo, R. Cammi, J. W. Ochterski, R. L. Martin, K. Morokuma, O. Farkas, J. B. Foresman and D. J. Fox, Journal, 2016.
2. A. V. Marenich, C. J. Cramer and D. G. Truhlar, *J Phys Chem B*, 2009, **113**, 6378-6396.
3. J. D. Chai and M. Head-Gordon, *Phys Chem Chem Phys*, 2008, **10**, 6615-6620
4. A. Schafer, C. Huber and R. Ahlrichs, *J Chem Phys*, 1994, **100**, 5829-5835.
5. S. Grimme, S. Ehrlich and L. Goerigk, *J Comput Chem*, 2011, **32**, 1456-1465.
6. Y. Minenkov, A. Singstad, G. Occhipinti and V. R. Jensen, *Dalton T*, 2012, **41**, 5526-5541.
7. A. D. Laurent and D. Jacquemin, *Int J Quantum Chem*, 2013, **113**, 2019-2039.
8. T. Lu and F. W. Chen, *J Comput Chem*, 2012, **33**, 580-592.
9. F. Neese, F. Wennmohs, U. Becker and C. Riplinger, *J Chem Phys*, 2020, **152**.
10. W. M. Haynes, CRC handbook of chemistry and physics. CRC press 2016.
11. R. Christian, T. Welton, Solvents and solvent effects in organic chemistry. John Wiley & Sons, 2011.
12. S. Emamian, T. Lu, H. Kruse, H. Emamian, *J. Comput. Chem.*, 2019, **40**, 2868-2881
13. W. Humphrey, A. Dalke and K. Schulten, *J Mol Graph Model*, 1996, **14**, 33-38.
14. N. B. Barhate, A. S. Gajare, R. D. Wakharkar, A. V. Bedekar, Tetrahedron, 1999, **55**, 11127-11142.
15. G. I. Nikishin, N. I. Kapustina, L. L. Sokova, O. V. Bityukov, A. O. Terent'ev, *RSC Adv.*, 2018, **8**, 28632-28636.
16. X. Cao, L. Wei, J. Yang, H. Song, Y. Wei, *Org. Biomol. Chem.*, 2024, **22**, 1157-1161.
17. J. Xu, Y. L. Zhang, X. G. Yue, J. Huo, D. K. Xiong, and P. F. Zhang, *Green Chem*. 2021, **23**, 5549-5555.
18. H. Huang, C. G. Yu, X. M. Li, Y. Q. Zhang, Y. T. Zhang, X. B. Chen, P. S. Mariano, H. X. Xie, and W. Wang, *Angew Chem Int Ed* 2017.56, 8201-8205.
19. Z. Bazyar, and M. Hosseini-Sarvari, *J. Org. Chem.* 2019, **84**, 13503-13515..
20. G. F. Zha, W. Y. Fang, J. Leng, and H. L. Qin, Adv. Synth. Catal. 2019, **361**, 2262-2267.
21. N. C. Jana, S. Behera, S. K. Maharana, R. R. Behera, and B. Bagh, *Catal. Sci. Technol.* 2023,**13**, 5422-5434.
22. R. R. Perrotta, A. H. Winter, W. H. Coldren, and D. E. Falvey. J. Am. Chem. Soc. 2011, **133**, 15553-15558.
23. M. Iinuma, K. Moriyama, and H. Togo *Eur. J. Org. Chem*. 2014, 772-780.
24. X. Z. Tian, Y. G. Guo, W. K. An, Y. L. Ren, Y. C. Qin, C. Y. Niu, and X. Zheng. *Nat. Commun.* 2022.**13**. 6186-6190.

25. C. Hu, V, C., Merchant, R. R., S. J. Chen, J. M. E. Hughes, B. K., Peters and T. Qin *J. Am. Chem. Soc.* 2023,**145**, 25-31.
26. X. P.,Jiang, G. Wang, Z. C. Zheng, X. H. Yu, Y. Hong, H. Q. Xia, and C. M. Yu, *Org. Lett.* 2020, **22**, 9762-9766.
27. W. Schilling, D. Riemer, Y. Zhang, N. Hatami, and S. Das, *ACS Catal.* 2018, **8**, 5425-5430.
28. K. Kobayashi, Y. Nishimura, F. X. Gao, K. Gotoh, Y. Nishihara, and K. Takagi. *J. Org. Chem.* 2011, **76**, 1949-1952.
29. K. Kim, S. Lee, and S. H. Hong *Org. Lett.* 2021. **23**, 5501-5505..
30. T. Fujihara, C. Cong, J. Terao, and Y. Tsuji *Adv. Synth. Catal.* 2013. **355**, 3420-3424.
31. B. Ardiansah, H. Tanimoto, T. Tomohiro, T. Morimoto, and K. Kakiuchi *Chem. Commun.* 2021, **57**, 8738-8741.